Diagrammatic Analysis for Parameterized Quantum Circuits

Tobias Stollenwerk
German Aerospace Center (DLR), Linder Höhe, 51147 Cologne, Germany
Institute for Quantum Computing Analytics (PGI-12), Jülich Research Centre, Wilhelm-Johnen-Straße, 52428 Jülich, Germany
tobias.stollenwerk@dlr.de

Stuart Hadfield
Quantum Artificial Intelligence Lab (QuAIL), NASA Ames Research Center, Moffett Field, CA 94035, USA
USRA Research Institute for Advanced Computer Science (RIACS), Mountain View, CA 94043, USA
stuart.hadfield@nasa.gov

Diagrammatic representations of quantum algorithms and circuits offer novel approaches to their design and analysis. In this work, we describe extensions of the ZX-calculus especially suitable for parameterized quantum circuits, in particular for computing observable expectation values as functions of or for fixed parameters, which are important algorithmic quantities in a variety of applications ranging from combinatorial optimization to quantum chemistry. We provide several new ZX-diagram rewrite rules and generalizations for this setting. In particular, we give formal rules for dealing with linear combinations of ZX-diagrams, where the relative complex-valued scale factors of each diagram must be kept track of, in contrast to most previously studied single-diagram realizations where these coefficients can be effectively ignored. This allows us to directly import a number useful relations from the operator analysis to ZX-calculus setting, including causal cone and quantum gate commutation rules. We demonstrate that the diagrammatic approach offers useful insights into algorithm structure and performance by considering several ansätze from the literature including realizations of hardware-efficient ansätze and QAOA. We find that by employing a diagrammatic representation, calculations across different ansätze can become more intuitive and potentially easier to approach systematically than by alternative means. Finally, we outline how diagrammatic approaches may aid in the design and study of new and more effective quantum circuit ansätze.

1 Introduction

Diagrammatic approaches to quantum mechanics [9, 13, 12] have gained much attention in recent years as an advantageous alternative approach to analyzing and understanding quantum systems, providing simpler intuition and in some cases improved algorithmic approaches. These methods provide straightforward rules for representing, manipulating, and simplifying quantum objects, while at the same time are underpinned by sophisticated mathematical ideas (in particular, category theory [1, 55]). An important example is the ZX-calculus [9, 10, 55] and its closely related variants [43, 51, 31, 35, 32, 3, 20] which have seen a number of successful applications in quantum computing, ranging from circuit optimization [19, 37, 4, 25] and synthesis [15, 26], to algorithm analysis [7, 49], natural language processing [11] and machine learning [57, 48, 58], among others.

In this paper we show how the ZX-calculus is also useful for analyzing algorithms based on parameterized quantum circuits (PQCs), such as variational quantum algorithms, in particular for calculating important derived quantities such as expectation values of quantum observables, or their gradients. Such quantities may be computed as functions of the circuit parameters, in which case the parameters are symbolically carried through subsequent ZX-diagrams, or as numbers for the case of fixed parameters

Submitted to:
QPL 2022

of interest. To enable this, we present several new ZX-rules generalizing the standard ones appearing in the literature; in particular, we present rules and notation for explicitly handling linear combinations of ZX-diagrams which naturally arise, for example, when incorporating commutation rules for unitary operators which are used for instance in computing expectation values. For linear combination of diagrams, clearly, it is critical to keep track of the scalar multiplier of each diagram, whereas in previous single-diagram applications such global phases or normalization constants can typically be ignored. In our application these multipliers will typically be complex-valued functions of the quantum circuit parameters. Furthermore, our formalism then allows direct importation of a number of useful relations from the operator analysis to ZX calculus setting, such as causal cone and operator commutation rules, among others.

After stating the new rules we demonstrate their efficacy with several prototypical examples of parameterized quantum circuits in the context of combinatorial optimization, including straightforward derivation of some new and existing results concerning example circuits drawn from the literature. While for computing expectation values of relatively shallow circuits we are able to show most of the key diagram reduction steps explicitly, for deeper circuits our approach can be aided by integration with software implementations of the ZX-calculus (e.g., [38, 36]). Though we focus on the common task of analyzing quantum circuit expectation values, important in particular for assessing algorithm performance, our proposed rules are general and may find much broader application in future work. For instance, toward analyzing phenomena related to parameter setting, expectation value gradients may be obtained either by differentiating directly [48], or by reducing the calculation to that of computing further circuit expectation values as in parameter shift rules [17, 56]. We emphasize that our approach may be applied to a wide variety of application problems and related quantum circuits beyond those explicitly considered in our examples, and further ZX results and generalizations from the literature may be leveraged, including extensions to qudits [51] or fermions [32, 16], among others.

2 Preliminaries

2.1 ZX-Calculus

We refer the reader to [50, 55] and the references therein for comprehensive introductions, including complete sets of graphical rewrite rules as well as their mathematical details. A number of the most important ZX-diagram rewrite rules are displayed in Figure 1. We use the label attached to each equation to reference these rules when we apply them in the examples we consider below.

2.2 Parameterized Quantum Circuits

Parameterized quantum circuits (PQC) have gained much attention in recent years, in particular as heuristic approaches suitable for NISQ [42] era devices that are classically optimized (often variationally) as part of a hybrid protocol, though we emphasize they are by no means restricted to this setting; see [8, 5] for reviews of recent developments. Two particular approaches of interest are the QAOA (quantum alternating operator ansatz [29], which generalizes the quantum approximate optimization algorithm [22]) and VQE (variational quantum eigensolver [41, 40]) paradigms, as well as a number of more recent variants of these approaches. Here we briefly review the original QAOA paradigm and its application to combinatorial optimization, though our results to follow may be applied more generally to a variety of problems and algorithms. In QAOA we are given a cost function $c(x)$ and corresponding classical Hamiltonian C (i.e., diagonal in the computational basis, $C|x\rangle = c(x)|x\rangle$) we seek to optimize over bit

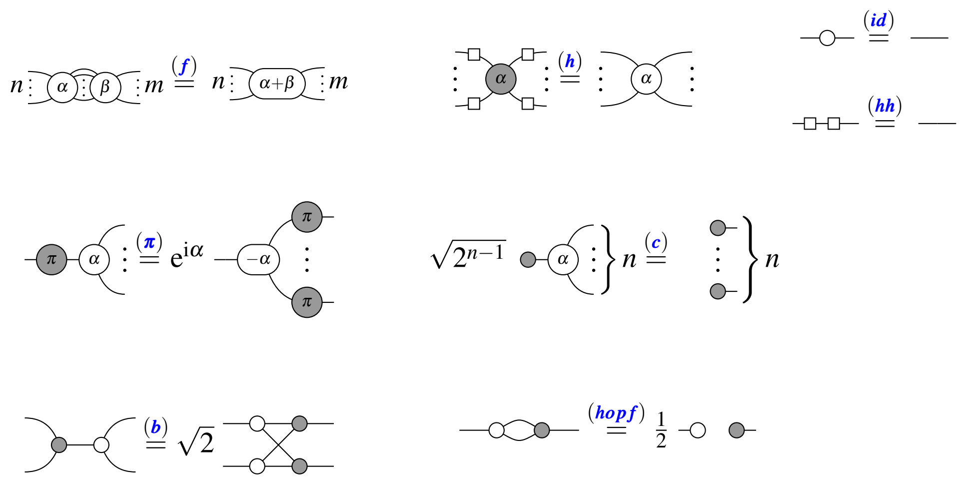

Figure 1: The ZX-diagram rewrite rules (cf. for example [55] or [58]). Note the explicit scalar factors.

strings $x \in \{0,1\}^n$. A QAOA$_p$ circuit consists of $2p$ alternating layers specified by $2p$ angles γ_i, β_i in some domain (e.g. $[-\pi, \pi]$) to create the state

$$|\boldsymbol{\gamma\beta}\rangle = U_M(\beta_p)U_P(\gamma_p)\dots U_M(\beta_1)U_P(\gamma_1)\,|s\rangle\ ,$$

for phase operator $U_P(\gamma) = \exp(-\mathrm{i}\gamma C)$, (transverse-field) mixing operator $U_M(\beta) = \exp(-\mathrm{i}\beta B)$ where $B = \sum_{i=1}^n X_i$, and standard initial product state $|s\rangle = |+\rangle^{\otimes n}$. The state is then measured in the computational basis which returns some $y \in \{0,1\}^n$ achieving cost $c(y)$. Figure 2 shows a simple example of a QAOA circuit. Repeated state preparation and measurement gives further samples which may be used to

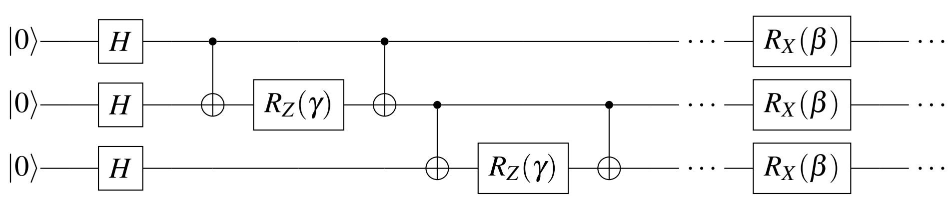

Figure 2: Example of a parameterized quantum circuit: QAOA on 3 qubits. Here the phase and mixing operators as well as initial state preparation have been compiled to basic quantum gates.

estimate the cost expectation $\langle C\rangle_p$ or other important quantities. These quantities may be used to update or search for better circuit parameters if desired; we emphasize that in different cases parameters may be found through analytic [53], numeric [22], or average-case [47] techniques, or, distinctly, searched for empirically (e.g., variationally). After a set number of runs overall, or when other suitable termination criteria has been reached, the best solution found is returned.

A fundamentally important quantity for QAOA as well as related approaches is the cost expectation value $\langle C\rangle$, which may be computed for a single instance or over a suitable class, and can be used to bound the expected approximation ratio achieved [22, 30, 29, 28] for the given problem. Importantly, we are often given a decomposition of the cost Hamiltonian such as $C = \sum_j C_j$ which we may exploit in computing $\langle C\rangle = \sum_j \langle C_j\rangle$ as a sum of terms (typically, a linear combination of Pauli Z operators [27]), which directly motivates the rules we introduce for accommodating linear combinations of ZX-diagrams. For combinatorial optimization the C_j terms mutually commute which leads to further simplifications, whereas this may not be true for more general problems and applications such as quantum chemistry (though linearity of expectation still applies). In general, many quantities of interest for PQCs can be expressed as expectation values and are hence amenable to similar analysis via diagrammatic techniques as we explore below.

2.3 Related Work

Several recent papers provide related but distinct results towards applying the ZX calculus in the PQC setting. In particular, three papers [48, 52, 34] which appeared during preparation of this work that consider differentiation and addition of ZX-diagrams. These papers introduce diagrammatic extensions complementary to our results. However they do not deal with expectation values explicitly which is the focus of this work. In terms of previous applications to variational quantum algorithms, a recent paper [58] considers using the ZX-calculus for computing and analyzing expectation values of derivatives of the cost expectation for particular classes of random parameterized quantum circuits built from particular gate sets (see in particular [58, Assumption 1]), in the context of detecting possible barren plateaus [39]. Our work differs in that we consider expectation values of the cost function themselves, and make no similar assumption of randomly selected parameters. A particular similarity with [58] is both their application and ours require explicit accounting of scalar factors associated to ZX-diagrams (see Section 3). However, while it is observed in [58, Eq. 7] that quantum expectation values may represented with the ZX-calculus in [58, Eq. 7], the authors do not apply the decomposition $C = \sum_j C_j$, which we exploit to derive novel ZX rules and analysis. Our approach and results are complementary to those of [58]. Another work [23] applied ZX-calculus in analysis of symmetries in the parameter landscape of the cost function expectation. We note that a different diagrammatic approach to constructing parameterized quantum circuits is considered in [33]. Concepts related to linear combinations of ZX-diagrams have been discussed in the framework of category theory for example in [14, 18].

3 ZX-Calculus for Parameterized Quantum Circuits

In this section we extend the ZX-calculus to accommodate linear combinations of (conventional) ZX-diagrams. Then, toward its application to parameterized quantum circuits we derive a collection of general rules and useful identities within the new framework. We will apply these rules to several concrete quantum circuit examples in Section 4 and the Appendices.

3.1 Diagrammatic Rules for Linear Combinations

Here we define linear combinations of diagrams, in which case diagram constants give the relative weights of the sum. For example, for computing the expectation value of an observable $H = \sum_{j=1}^{m} a_j H_j$ for some quantum circuit state $|\psi\rangle = U\,|\psi_0\rangle$ we have $\langle H\rangle_\psi = \sum_{j=1}^{m} a_j \langle H_j\rangle_\psi$, which hence corresponds to a single ZX-diagram or equivalently to a sum of m weighted diagrams. This idea generalizes in the natural way to sums of linear maps and more general ZX objects. We also show new ZX-diagram rules which relate single (sub)diagrams to sums or products of (sub)diagrams, such that the resulting diagram reductions involve differing numbers of diagrams.

As mentioned, we do not use the common convention of considering diagrams equivalent up to scalars or phases; hence we include complex scalar multipliers explicitly in our diagrams and rules to follow, i.e.,

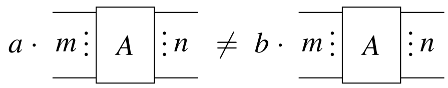

unless $a = b$,

where a, b are complex scalar multipliers and the diagram is a placeholder for an arbitrary ZX-diagram with m inputs and n outputs. In particular, care must be taken in applying the usual rules of ZX-calculus to account for any implicit constant factors. We note that scalar factors are also retained in the distinct application of [58]; see [58, Fig. 4] for an example list of some ZX-diagram rewrite rules with explicit scalars.

Definition 3.1 (Sum notation)**.** We define novel diagram notation for describing arbitrary linear combinations. The linear combination of two ZX-diagrams with m inputs and n outputs is written

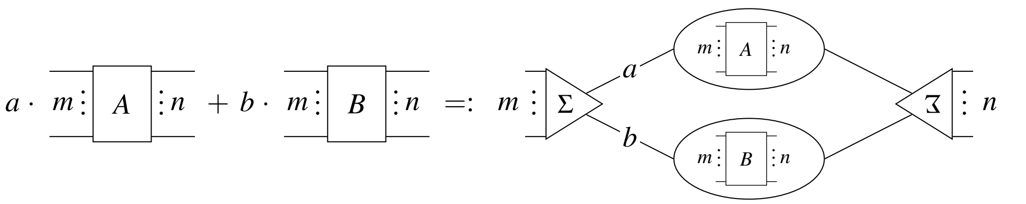

(1)

Each summand is written inside a *bubble* and the scalar factors are written on the line combining the new summation symbol and the bubbles. This definition naturally extends to an arbitrary number of summands. Summand diagrams are required have the same numbers of input (m) and output (n) lines as each other and as the those of the sum object. Note that m or n are zero for diagrams representing states $(m = 0)$, effects $(n = 0)$, or constants $(m = n = 0)$. Sums of diagrams also arise in [57, 48, 58] in the context of differentiating diagram components (where sums arise, for example, from the product rule of calculus). Our work is complementary to these results in that we consider the generalization to complex linear combinations of diagrams; extensions to scalars beyond the complex numbers are also possible [48].

3.1.1 Rules

Now we state the two rules needed for the extension of ZX-calculus to linear combinations.

1. Diagram Pull Rule

   The first rule applies if diagrams in a linear combination are equal up to a certain subdiagram (A and B below). Then we can write a single diagram containing the linear combination of the beforementioned subdiagrams

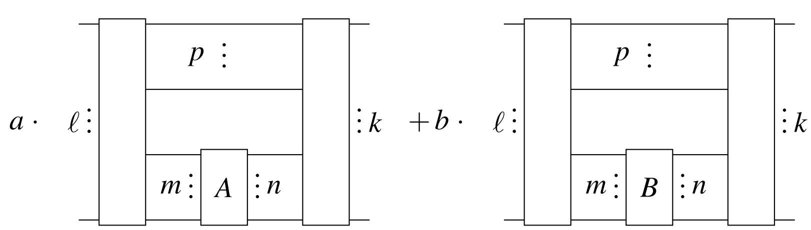

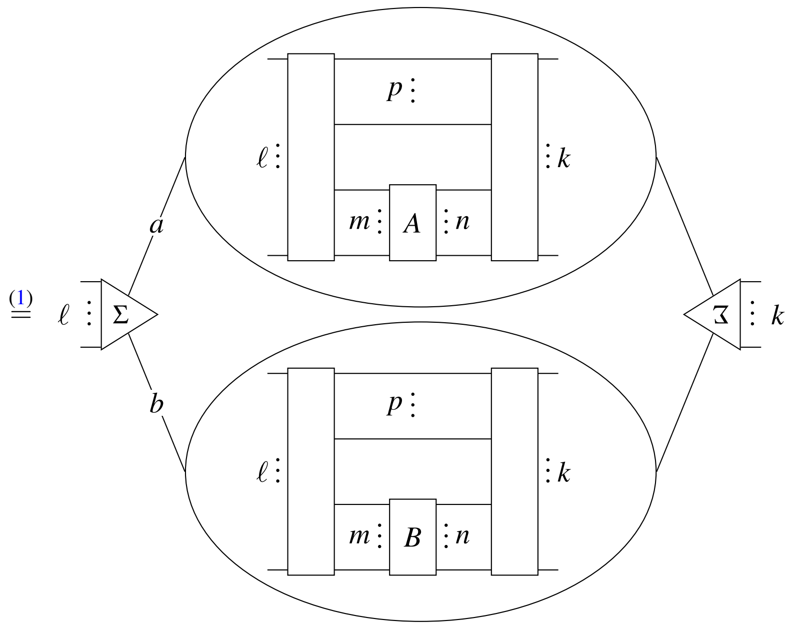

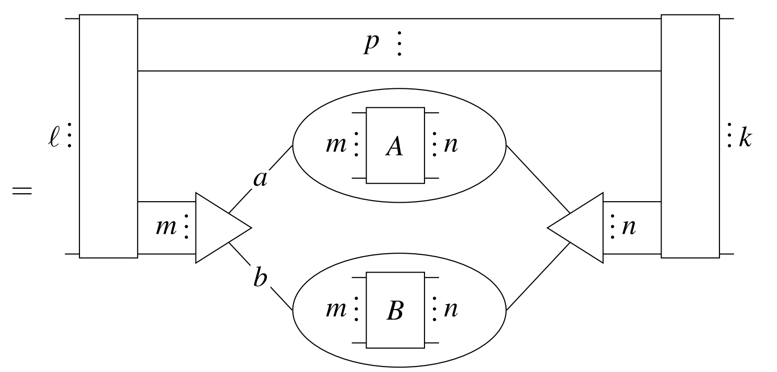

(i)

The last equality we call the *diagram pull rule*. This also holds if any of the ℓ, p, k, m, n vanish. Thus describing how to pull scalars, effects and states in and out of the bubbles. If $p = 0$, the rule describes how to pull in and out diagrams only from the left or only from the right. We will make heavy use of this in Section 4.

2. Product (Composition) Rule

   The second rule describes how to combine products (i.e., compositions) of linear combinations of diagrams. We state the rule for a product of two linear combinations comprised of two summands each

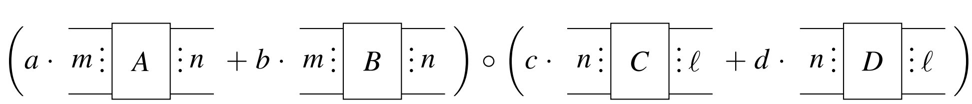

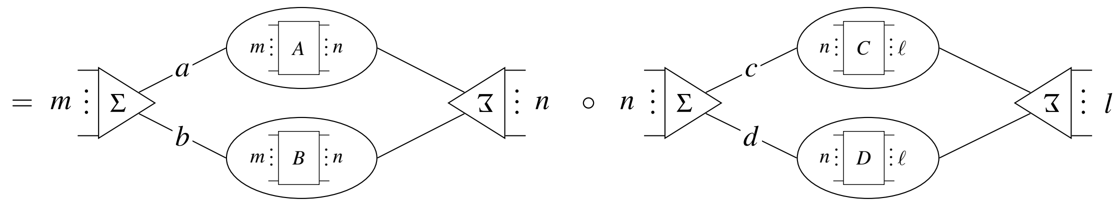

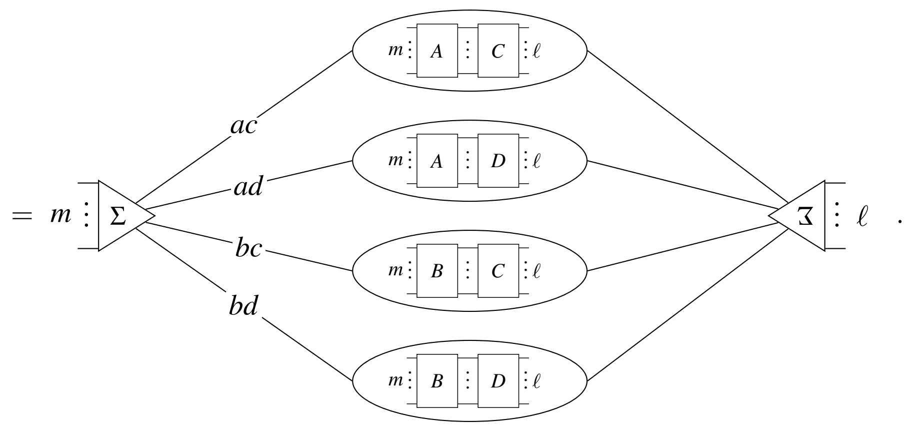

(ii)

The product rule extends in the obvious way to the case of more than two factors or summands. Several additional rules are given in Appendix A.

3.2 ZX-Calculus for Expectation Values of Quantum Circuits

In this section, we will present various identities within the extended ZX-calculus framework, that are useful for the analysis of parameterized quantum circuits. While we primarily consider Pauli operators here, similar results may derived in different basis or gate sets. See [16] for some additional useful rules regarding Pauli operator exponentials.

3.2.1 Rotations

First, we can write rotation operators in terms of linear combinations of Clifford gates

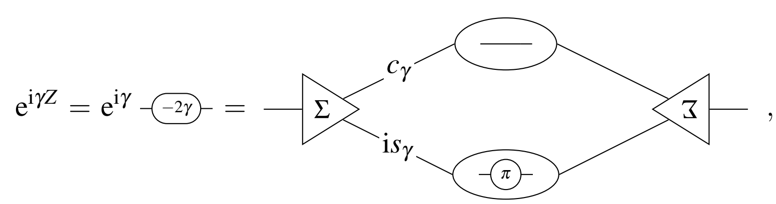

(5)

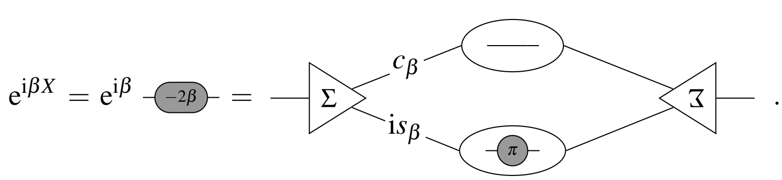

(6)

In both cases the proof easily follows from the identity $e^{i\alpha A} = \cos\alpha I + i\sin\alpha A$ for operators satisfying $A^2 = I$. We use $c_\alpha := \cos(\alpha)$ and $s_\alpha := \sin(\alpha)$ throughout.

3.2.2 Phase-Gadgets

Important for parameterized quantum circuits are multi-qubit rotations, so-called *phase-gadgets* (cf. [16]), for example

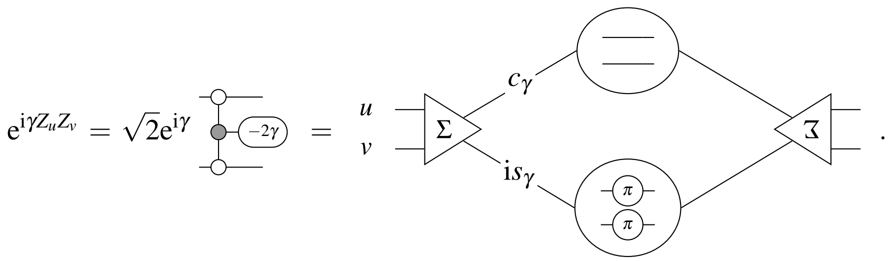

(7)

A proof of the first equality is given in [16, Corollary 3.4]. The second equality is derived similarly to (5), (6). In particular, for the analysis of QAOA expectation values, we will encounter conjugates of phase-gadgets in conjunction with π-X-spiders. We will make heavy use of the following identity which is proven in Appendix D.1.

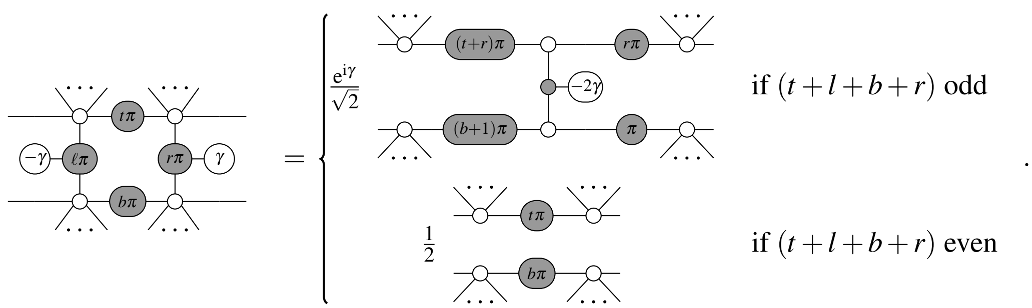

(8)

Phase-gadgets can be combined to implement so-called *phase polynomials*, i.e., parameterized exponentials of diagonal Hamiltonians such as utilized in QAOA circuits [26, 16, 29, 27].

3.2.3 Lightcones

For quantum circuits of limited depth or connectivity, it is often the case when computing a particular quantity that a significant fraction of the gates and qubits can be ignored or discarded due to having no effect, in analogy with spacelike-separated events in relativity. Naturally, the same principle may be fruitfully applied to diagrammatic analysis.

Given an observable $C = \sum_j C_j$, typically each C_j acts nontrivially on a subset of $\ell < n$ qubits. Hence, depending on the structure of the problem and given quantum circuit ansatz $U|\psi_0\rangle$, the n-qubit expectation values $\langle C_j \rangle$ may be equivalently reduced to ones over L qubits, $\ell \leq L \leq n$, by in each case restricting the quantum circuit in the natural way. This phenomena is generally known as the *lightcone* or *causal cone* rule [21, 22, 47, 28], and is clearly exhibited with the ZX-calculus. For example, if $|\psi_0\rangle$ is a product state and U consists of only 1-local gates, then $L = \ell$ independently of the circuit depth (cf. the example of Section 4.1). For QAOA applied to MaxCut, $\ell = 2$ and it is easily shown that the lightcone after each qth QAOA layer consists of the restriction to the subgraph within distance q of the given edge [22, 28], i.e., its size L depends on the vertex degrees in the graph neighborhood. Hence, importantly, for QAOA or similar layered ansatz we may apply the lightcone rule layer-by-layer. Applying this restriction, the inner operator for a MaxCut QAOA expectation value reads

$$\mathscr{O}^p_{uv} := \prod_{\ell=1}^{p} \mathrm{e}^{\mathrm{i}\gamma_\ell C} \mathrm{e}^{\mathrm{i}\tilde{\beta}_\ell B} Z_u Z_v \prod_{k=p}^{1} \mathrm{e}^{-\mathrm{i}\tilde{\beta}_k B} \mathrm{e}^{-\mathrm{i}\gamma_k C}$$

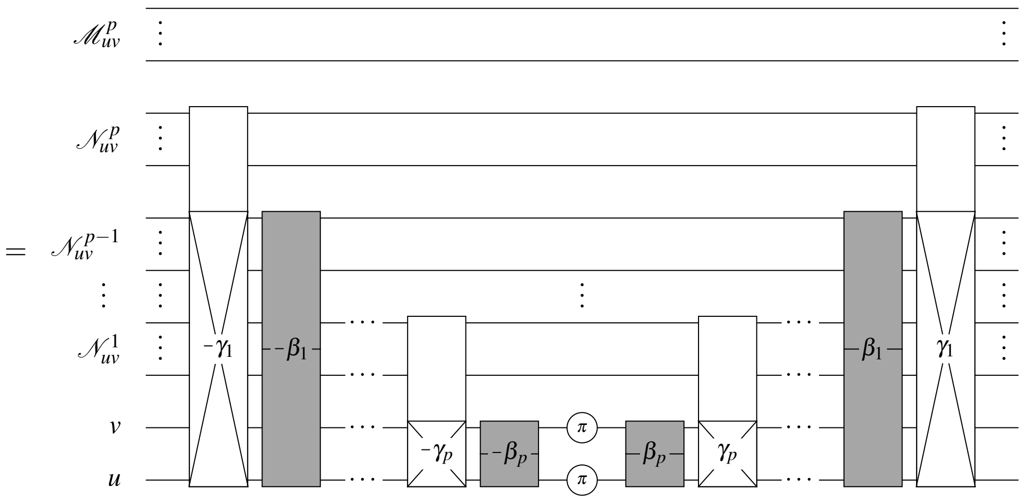

, (9)

where we used placeholder diagrams for the *reduced* phase-separation layer

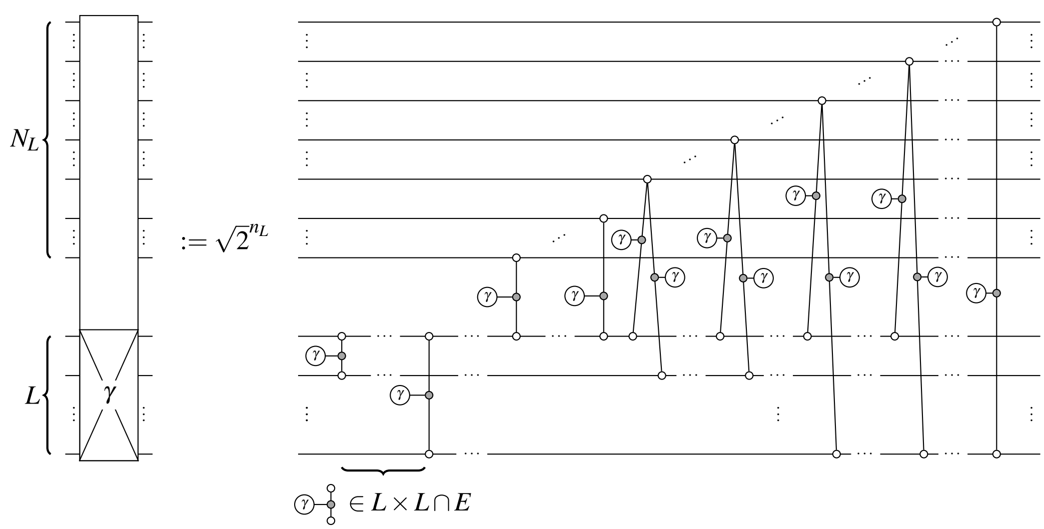

, (10)

and the *reduced* mixing layer

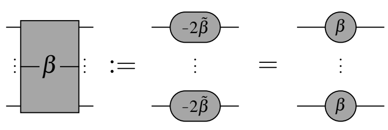

(11)

where $\beta := -2\tilde{\beta}$ for convenience. For the reduced phase-separation layer we have used the MaxCut cost function Hamiltonian $C = \frac{1}{2}\sum_{uv\in E}(1 - Z_u Z_v)$ and

$$\mathrm{e}^{\mathrm{i}\gamma C} = \prod_{(u,v)\in E} \mathrm{e}^{\frac{\mathrm{i}\gamma}{2}} \mathrm{e}^{\frac{-\mathrm{i}\gamma}{2} Z_u Z_v} \overset{(7)}{=} \sqrt{2}^{|E|} \prod_{(u,v)\in E}$$ 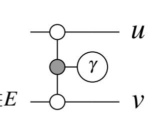

.

This leads to the factor $\sqrt{2}^{n_L}$ in (10), where n_L is the number of phase-gadgets in the right diagram of (10). Also, we implicitly used the neighborhood of a set of nodes L, $N_L := \bigcup_{\ell \in L} \mathrm{nbhd}(\ell)$, the exclusive p-th neighborhood of $\{u,v\}$, recursively defined by

$$\mathcal{N}_{uv}^{p} := \bigcup_{i,j \in \mathcal{N}_{uv}^{p-1} \times \mathcal{N}_{uv}^{p-1} \cap E} N_{\{i,j\}} \setminus \cup_{k=0}^{p-1} \mathcal{N}_{uv}^{k},$$

where $\mathcal{N}_{uv}^{0} := \{u,v\}$, as well as the complement $\mathcal{M}_{uv}^{p} = \mathcal{N}_{uv}^{p} \setminus E$.

While here we have considered QAOA circuits as a demonstrative example, the same principle may be applied to or formalized for more general ansätze and observables.

4 Application to Combinatorial Optimization

Expectation values of quantum circuit observables – i.e., constants – may be represented with ZX-diagrams, as has been previously observed in [58, Eq. 7]. In doing so, in some cases the structure of the original problem may be directly reflected in the structure of the corresponding ZX-diagrams. This is demonstrated by two examples in this section, in which apply our ZX-calculus extension to calculate cost expectation values for a particular ansatz for combinatorial optimization. The purpose of this section is twofold. First, we want to demonstrate that calculations with parameterized quantum circuits, like the finding an analytical expression for expectation values, can sometimes become more intuitive and simplified by using ZX-calculus in conjunction with our extension to linear combinations. Second, we show that our extension is indeed necessary to achieve the aforementioned task diagrammatically by, for instance, providing means to "commute" X- and Z-spiders (cf. (12)), while explicitly keeping track of all resulting terms.

We show how the cost function expectation value $\langle C \rangle$ may be computed and analyzed using our extended ZX-calculus. Recall that given a decomposition of the cost Hamiltonian $C = \sum C_\ell$ it suffices to compute the $\langle C_\ell \rangle$ values independently, which typically correspond to similar diagrams. In particular (sub)graph symmetry can be exploited to reduced the number of unique diagrams required [22, 44, 45]. Generally the quantity $\langle C \rangle$ is important in parameter setting, as well as bounding algorithm performance such as the approximation ratio achieved [30].

4.1 Independent Single-Qubit Rotations Ansatz

We begin with a simple but important example. Consider an arbitrary cost function and corresponding cost (diagonal) Hamiltonian C on n qubits we seek to extremize, together with the simple depth-1 ansatz consisting of a free single-qubit Pauli-Y rotation on each qubit, applied to the initial state $|00\ldots0\rangle = |0\rangle^{\otimes n}$,

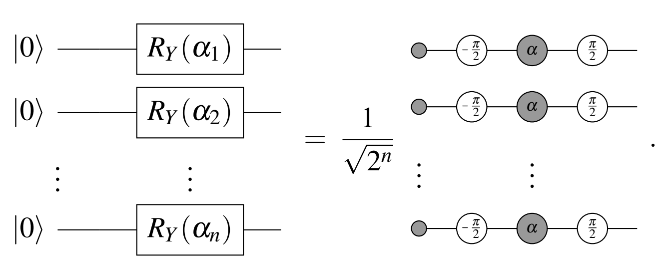

For example, consider an arbitrary instance of MaxCut, a prototypical NP-hard optimization problem, though the same argument we show here applies similarly to many other problems. For a graph with edge set E the cost Hamiltonian is $C = \frac{|E|}{2} - \frac{1}{2}\sum_{(uv)\in E} Z_u Z_v$. As demonstrated in Equation (12) the derivation of each $\langle Z_u Z_v \rangle$ becomes very simple with ZX-calculus.

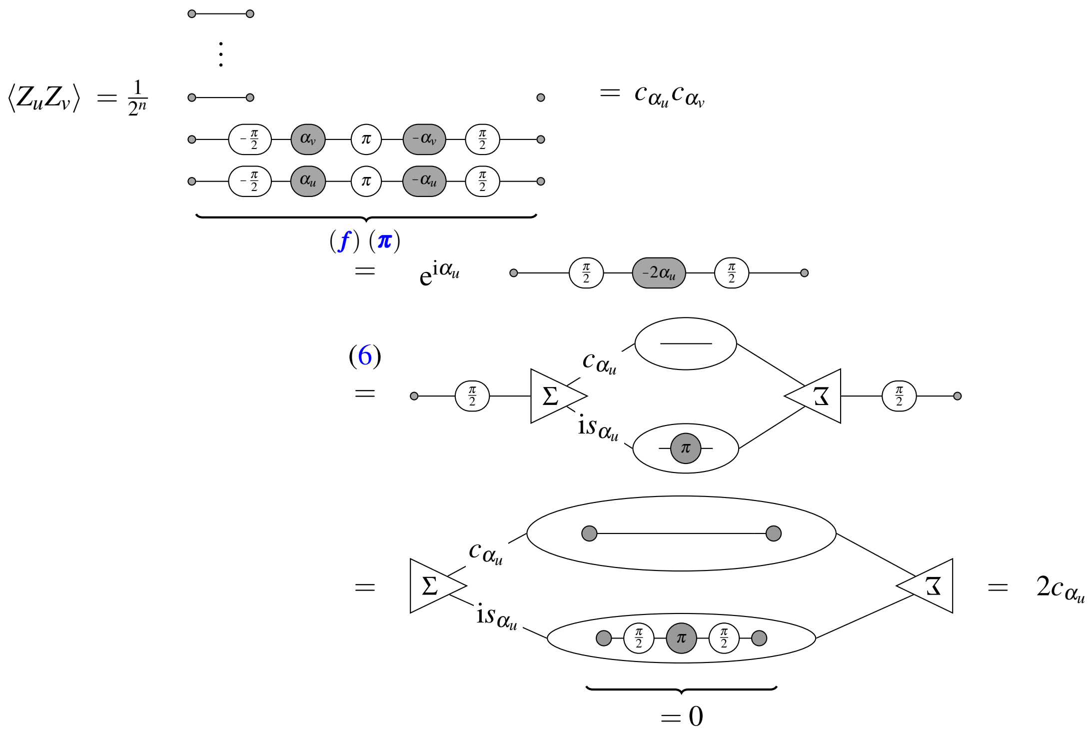

. (12)

Here, again, $s_\alpha = \sin(\alpha)$ and $c_\alpha = \cos(\alpha)$, and each underbrace used refers only to the subdiagram directly above. Note that after the second step the usage of linear combinations to handle the X-spider with phase $(-2\alpha_u)$ provides a way to continue the calculation, which would not be possible within the conventional ZX-framework. From the permutation symmetry of the ansatz, the expectation value $\langle Z_i Z_j \rangle$ of each edge is of the same form [44]. Hence we have

$$\langle C \rangle = \frac{|E|}{2} - \frac{1}{2} \sum_{(u,v)\in E} \cos(\alpha_u)\cos(\alpha_v), \tag{13}$$

which implies

$$\max_{\alpha} \langle C \rangle = \max_{\alpha \in \{0,\pi\}^n} \langle C \rangle = \max_x c(x) = c(y^*),$$

where we have used the observation that angles $\alpha^* \in \{0,\pi\}^n$ encode a bit string y^* via $y_i^* = \frac{1}{2} - \frac{1}{2}\cos(\alpha_i^*)$. Hence, as any globally optimal angles must directly encode an optimal solution to the MaxCut instance, the expectation value $\langle C \rangle$ is NP-hard to optimize. Indeed, for MaxCut, (13) reproduces the quantity of Equation 1 of [6] (up to an affine shift). This result is used throughout [6] via further reductions to show that optimizing a number of other classes of PQCs is NP-hard in general. We have similarly demonstrated that the single-qubit rotations ansatz is NP-hard to optimize for problems such as MaxCut, but via a compact derivation using ZX-diagrams.

4.2 QAOA$_1$ for MaxCut on a Simple Graph

Next we turn to QAOA [22, 29], for which we continue our use of MaxCut as a running example. For simplicity we consider QAOA$_1$, the lowest depth realization, which is indicative of the $p > 1$ case due to the alternating structure of the ansatz. Recall that for a QAOA state the MaxCut expectation value reads $\langle C\rangle = \frac{|E|}{2} - \frac{1}{2}\sum_{i,j\in E}\langle Z_i Z_j\rangle$. We begin with the specific graph G of Figure 3, before we consider ring graphs in Section B.2, and arbitrary graphs in Appendix B.3. Observe how the structure of the graph

$G =$ 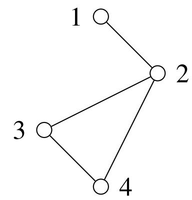

Figure 3: Simple example graph to consider for MaxCut with QAOA

directly reappears in the diagrams below, which reflects the fact that the QAOA phase operator is derived from the cost Hamiltonian. For deeper QAOA circuits, the graph structure will again appear at each layer in the diagrammatic representation. Hence ZX-calculus provides a toolkit toward directly incorporating or better understanding the relationship between the cost function and a given parameterized quantum algorithm.

Here we demonstrate the edge expectation value calculation for QAOA_1,

$\langle Z_2 Z_3\rangle_{\mathrm{QAOA}_1} = \frac{2^4}{2^4}$ 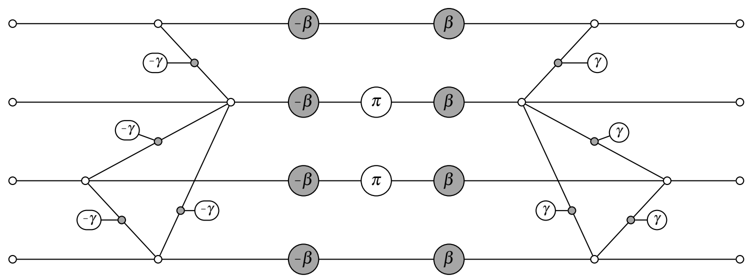

$\overset{(f)(\pi)}{=}$ $\mathrm{e}^{-2i\beta}$ 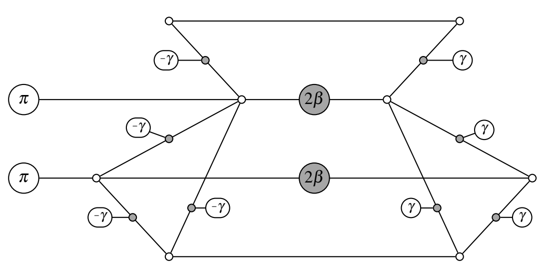

$\overset{(6)}{=}$ 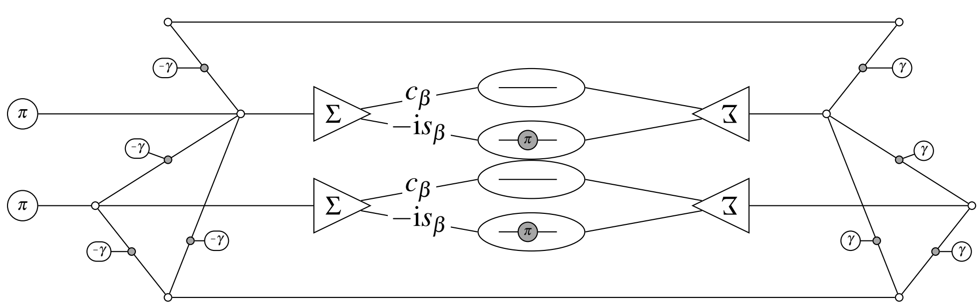

$\overset{(i)\,(ii)}{=}$

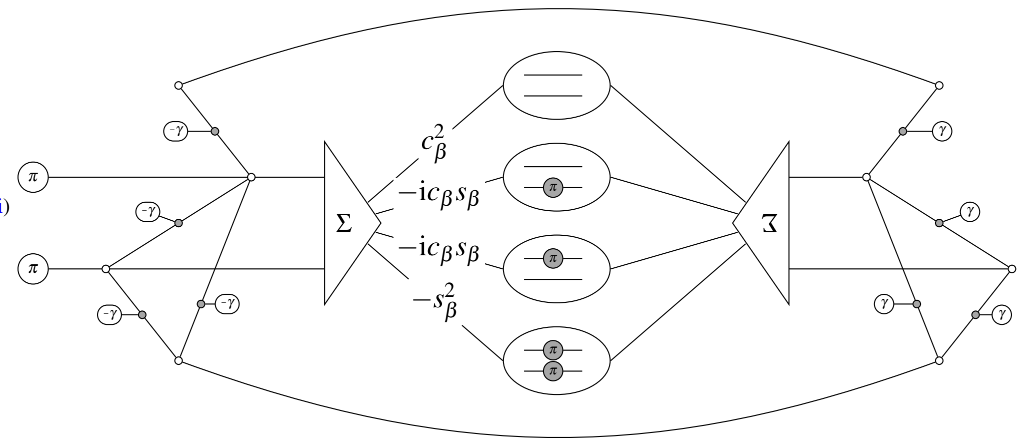

$\overset{(i)}{=}$

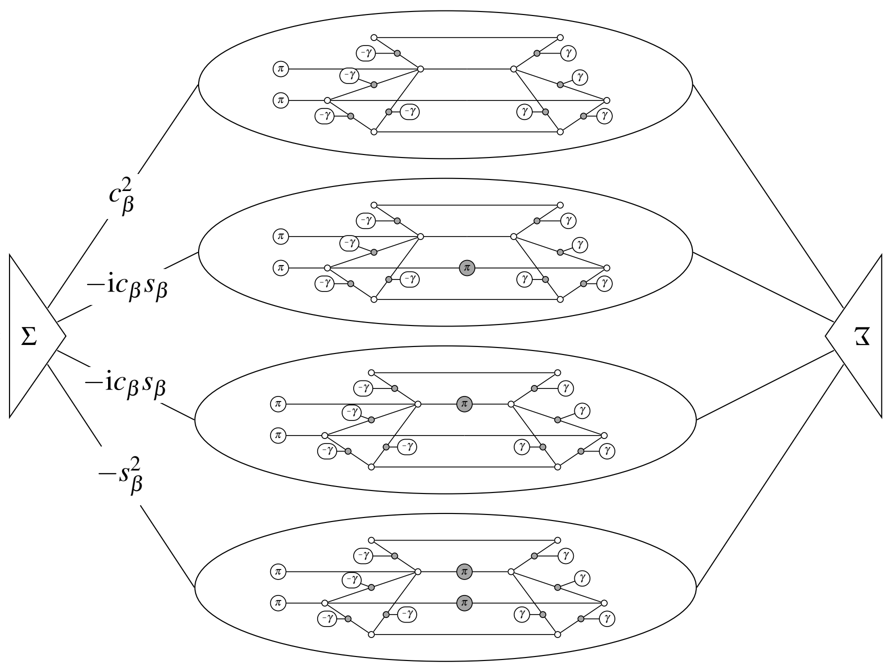

(14)

$\overset{(20)(21)(22)(23)}{=}$

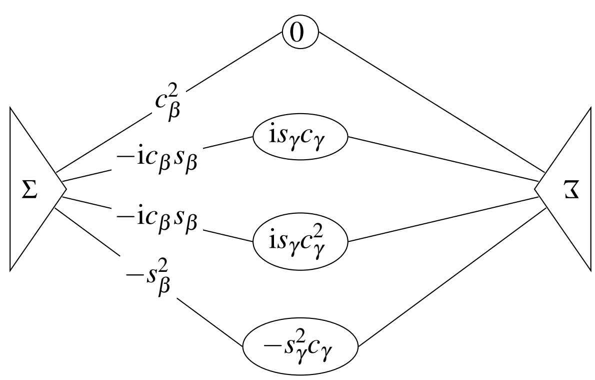

$$= \quad c_\beta s_\beta s_\gamma c_\gamma + c_\beta s_\beta s_\gamma c_\gamma^2 + s_\beta^2 s_\gamma^2 c_\gamma \quad .$$

The remaining expectation values can be similarly computed for each of the edges in E to give $\langle C \rangle$. In the third step above, we could not have easily continued within the conventional ZX-calculus framework. Whenever one needs to pull parameterized X-spiders through parameterized Z-spiders or vice versa, our extension is utilized. The detailed calculation of the four contributions used in the last step is given in Appendix C. Note that calculation of the general n-qubit case (cf. Appendix B.3) is surprisingly concise compared to the special case of 4-qubits considered here.

We consider a hardware-efficient ansatz and two more general QAOA examples in Appendix B.

5 Outlook

We introduced an extension of the ZX-calculus to conveniently incorporate linear combinations of ZX-diagrams. Moreover we demonstrated how this generalized diagrammatic framework can be applied to the analysis of parameterized quantum circuits, in particular to the calculation of observable expectation values. Further quantities of interest such as gradients may be similarly derived, as well as more complicated PQC phenomenon such as barren plateaus studied, by combining our framework with several distinct but complementary recent ZX-calculus advances [58, 34, 52]. Software implementation of these results may facilitate novel approaches for automatic contraction of diagrams related to PQCs, including but not limited to expectation values. A concrete next step is to rigorously derive such algorithms and carefully analyze problems and PQC classes where they may yield advantages.

Future research could further formalize our approach as well as integrate it with other variants of ZX-calculus, like ZH-calculus [3] or the ZX-framework for qudits [43, 51]. In particular the latter could facilitate novel insights into performance analysis of quantum alternating operator ansätze [29] for problems like graph-coloring [54] and beyond [46]. Similarly, our approach could be likewise applied to applications beyond combinatorial optimization, like variational quantum eigensolvers for quantum chemistry applications [16]. Generally, it is of interest to explore to what extent diagrammatic approaches may ultimately aid in the design and analysis of better performing parameterized quantum circuit ansätze, as well as help with important related challenges such as alleviating the cost of parameter setting, avoiding undesirable features such as barren plateaus, or tailoring ansatz design to a given set of hardware constraints.

Acknowledgments

SH is grateful for support from the NASA Ames Research Center, from NASA Academic Mission Services (NAMS) under Contract No. NNA16BD14C, and from the DARPA ONISQ program under inter-agency agreement IAA 8839, Annex 114.

References

[1] Samson Abramsky & Bob Coecke (2004): *A categorical semantics of quantum protocols*. In: *Proceedings of the 19th Annual IEEE Symposium on Logic in Computer Science, 2004.*, IEEE, pp. 415–425.

[2] Gadi Aleksandrowicz et al. (2019): *Qiskit: An Open-source Framework for Quantum Computing*, doi:10.5281/zenodo.2562111. Available at `https://qiskit.org/documentation/stubs/qiskit.circuit.library.EfficientSU2.html`.

[3] Miriam Backens & Aleks Kissinger (2019): *ZH: A Complete Graphical Calculus for Quantum Computations Involving Classical Non-linearity*. In Peter Selinger & Giulio Chiribella, editors: Proceedings

of the 15th International Conference on *Quantum Physics and Logic*, Halifax, Canada, 3-7th June 2018, *Electronic Proceedings in Theoretical Computer Science* 287, Open Publishing Association, pp. 23–42, doi:10.4204/EPTCS.287.2. Available at https://arxiv.org/abs/1805.02175.

[4] Miriam Backens, Hector Miller-Bakewell, Giovanni de Felice, Leo Lobski & John van de Wetering (2021): *There and back again: A circuit extraction tale*. *Quantum* 5, p. 421, doi:10.22331/q-2021-03-25-421. Available at https://doi.org/10.22331/q-2021-03-25-421.

[5] Kishor Bharti, Alba Cervera-Lierta, Thi Ha Kyaw, Tobias Haug, Sumner Alperin-Lea, Abhinav Anand, Matthias Degroote, Hermanni Heimonen, Jakob S Kottmann, Tim Menke et al. (2022): *Noisy intermediate-scale quantum algorithms*. *Reviews of Modern Physics* 94(1), p. 015004.

[6] Lennart Bittel & Martin Kliesch (2021): *Training variational quantum algorithms is NP-hard*. *Physical Review Letters* 127(12), p. 120502.

[7] Titouan Carette, Yohann D'Anello & Simon Perdrix (2021): *Quantum Algorithms and Oracles with the Scalable ZX-calculus*. In Chris Heunen & Miriam Backens, editors: Proceedings 18th International Conference on *Quantum Physics and Logic*, Gdansk, Poland, and online, 7-11 June 2021, *Electronic Proceedings in Theoretical Computer Science* 343, Open Publishing Association, pp. 193–209, doi:10.4204/EPTCS.343.10. Available at https://arxiv.org/abs/2104.01043.

[8] Marco Cerezo, Andrew Arrasmith, Ryan Babbush, Simon C Benjamin, Suguru Endo, Keisuke Fujii, Jarrod R McClean, Kosuke Mitarai, Xiao Yuan, Lukasz Cincio et al. (2021): *Variational quantum algorithms*. *Nature Reviews Physics* 3(9), pp. 625–644.

[9] Bob Coecke & Ross Duncan (2008): *Interacting quantum observables*. In: *International Colloquium on Automata, Languages, and Programming*, Springer, pp. 298–310. Available at https://arxiv.org/abs/0906.4725.

[10] Bob Coecke & Ross Duncan (2011): *Interacting quantum observables: categorical algebra and diagrammatics*. *New Journal of Physics* 13(4), p. 043016, doi:10.1088/1367-2630/13/4/043016. Available at https://doi.org/10.1088/1367-2630/13/4/043016.

[11] Bob Coecke, Giovanni de Felice, Konstantinos Meichanetzidis & Alexis Toumi (2020): *Foundations for Near-Term Quantum Natural Language Processing*. *arXiv preprint arXiv:2012.03755*.

[12] Bob Coecke, Dominic Horsman, Aleks Kissinger & Quanlong Wang (2021): *Kindergarden quantum mechanics graduates (... or how I learned to stop gluing LEGO together and love the ZX-calculus)*. *arXiv preprint arXiv:2102.10984*.

[13] Bob Coecke & Aleks Kissinger (2017): *Picturing Quantum Processes: A First Course in Quantum Theory and Diagrammatic Reasoning*. Cambridge University Press, doi:10.1017/9781316219317.

[14] Cole Comfort, Antonin Delpeuch & Jules Hedges (2020): *Sheet diagrams for bimonoidal categories*. *arXiv preprint arXiv:2010.13361*. Available at https://arxiv.org/abs/2010.13361.

[15] Alexander Cowtan, Silas Dilkes, Ross Duncan, Will Simmons & Seyon Sivarajah (2020): *Phase Gadget Synthesis for Shallow Circuits*. In Bob Coecke & Matthew Leifer, editors: Proceedings 16th International Conference on *Quantum Physics and Logic*, Chapman University, Orange, CA, USA., 10-14 June 2019, *Electronic Proceedings in Theoretical Computer Science* 318, Open Publishing Association, pp. 213–228, doi:10.4204/EPTCS.318.13. Available at https://arxiv.org/abs/1906.01734.

[16] Alexander Cowtan, Will Simmons & Ross Duncan (2020): *A Generic Compilation Strategy for the Unitary Coupled Cluster Ansatz*. *arXiv preprint arXiv:2007.10515*. Available at https://arxiv.org/abs/2007.10515.

[17] Gavin E Crooks (2019): *Gradients of parameterized quantum gates using the parameter-shift rule and gate decomposition*. *arXiv preprint arXiv:1905.13311*.

[18] Ross Duncan (2009): *Generalized Proof-Nets for Compact Categories with Biproducts*, p. 70–134. Cambridge University Press, doi:10.1017/CBO9781139193313.004.

[19] Ross Duncan, Aleks Kissinger, Simon Perdrix & John van de Wetering (2020): *Graph-theoretic simplification of quantum circuits with the ZX-calculus*. Quantum 4, p. 279, doi:10.22331/q-2020-06-04-279. Available at https://doi.org/10.22331/q-2020-06-04-279.

[20] Richard DP East, John van de Wetering, Nicholas Chancellor & Adolfo G Grushin (2022): *AKLT-states as ZX-diagrams: Diagrammatic reasoning for quantum states*. PRX Quantum 3(1), p. 010302.

[21] Glen Evenbly & Guifré Vidal (2009): *Algorithms for entanglement renormalization*. Physical Review B 79(14), p. 144108.

[22] Edward Farhi, Jeffrey Goldstone & Sam Gutmann (2014): *A quantum approximate optimization algorithm*. arXiv preprint arXiv:1411.4028. Available at https://arxiv.org/abs/1411.4028.

[23] Enrico Fontana, M Cerezo, Andrew Arrasmith, Ivan Rungger & Patrick J Coles (2020): *Optimizing parametrized quantum circuits via noise-induced breaking of symmetries*. arXiv preprint arXiv:2011.08763.

[24] Lena Funcke, Tobias Hartung, Karl Jansen, Stefan Kühn & Paolo Stornati (2021): *Dimensional Expressivity Analysis of Parametric Quantum Circuits*. Quantum 5, p. 422, doi:10.22331/q-2021-03-29-422. Available at https://doi.org/10.22331/q-2021-03-29-422.

[25] Jonathan Gorard, Manojna Namuduri & Xerxes D Arsiwalla (2021): *ZX-Calculus and Extended Wolfram Model Systems II: Fast Diagrammatic Reasoning with an Application to Quantum Circuit Simplification*. arXiv preprint arXiv:2103.15820. Available at https://arxiv.org/abs/2103.15820.

[26] Arianne Meijer-van de Griend & Ross Duncan (2020): *Architecture-aware synthesis of phase polynomials for NISQ devices*. arXiv preprint arXiv:2004.06052. Available at https://arxiv.org/abs/2004.06052.

[27] Stuart Hadfield (2021): *On the representation of Boolean and real functions as Hamiltonians for quantum computing*. ACM Transactions on Quantum Computing 2(4), pp. 1–21.

[28] Stuart Hadfield, Tad Hogg & Eleanor G Rieffel (2021): *Analytical Framework for Quantum Alternating Operator Ansätze*. arXiv preprint arXiv:2105.06996.

[29] Stuart Hadfield, Zhihui Wang, Bryan O'Gorman, Eleanor G. Rieffel, Davide Venturelli & Rupak Biswas (2019): *From the Quantum Approximate Optimization Algorithm to a Quantum Alternating Operator Ansatz*. Algorithms 12(2), doi:10.3390/a12020034. Available at https://www.mdpi.com/1999-4893/12/2/34.

[30] Stuart Andrew Hadfield (2018): *Quantum algorithms for scientific computing and approximate optimization*. Columbia University. Available at https://arxiv.org/abs/1805.03265.

[31] Amar Hadzihasanovic (2015): *A Diagrammatic Axiomatisation for Qubit Entanglement*. In: Proceedings of the 2015 30th Annual ACM/IEEE Symposium on Logic in Computer Science (LICS), LICS '15, IEEE Computer Society, USA, p. 573–584, doi:10.1109/LICS.2015.59. Available at https://doi.org/10.1109/LICS.2015.59.

[32] Amar Hadzihasanovic, Giovanni de Felice & Kang Feng Ng (2018): *A Diagrammatic Axiomatisation of Fermionic Quantum Circuits*. In Hélène Kirchner, editor: 3rd International Conference on Formal Structures for Computation and Deduction (FSCD 2018), Leibniz International Proceedings in Informatics (LIPIcs) 108, Schloss Dagstuhl–Leibniz-Zentrum fuer Informatik, Dagstuhl, Germany, pp. 17:1–17:20, doi:10.4230/LIPIcs.FSCD.2018.17. Available at http://drops.dagstuhl.de/opus/volltexte/2018/9187.

[33] Y Herasymenko & TE O'Brien (2021): *A diagrammatic approach to variational quantum ansatz construction*. Quantum 5, p. 596.

[34] Emmanuel Jeandel, Simon Perdrix & Margarita Veshchezerova (2022): *Addition and Differentiation of ZX-diagrams*. arXiv preprint arXiv:2202.11386. Available at https://arxiv.org/abs/2202.11386.

[35] Emmanuel Jeandel, Simon Perdrix & Renaud Vilmart (2018): *Y-Calculus: A Language for Real Matrices Derived from the ZX-Calculus*. In Bob Coecke & Aleks Kissinger, editors: Proceedings 14th International Conference on Quantum Physics and Logic, Nijmegen, The Netherlands, 3-7 July 2017, Electronic Proceedings in Theoretical Computer Science 266, Open Publishing Association, pp. 23–57, doi:10.4204/EPTCS.266.2. Available at https://arxiv.org/abs/1702.00934.

[36] Aleks Kissinger & John van de Wetering (2020): *PyZX: Large Scale Automated Diagrammatic Reasoning*. In Bob Coecke & Matthew Leifer, editors: Proceedings 16th International Conference on *Quantum Physics and Logic*, Chapman University, Orange, CA, USA., 10-14 June 2019, *Electronic Proceedings in Theoretical Computer Science* 318, Open Publishing Association, pp. 229–241, doi:10.4204/EPTCS.318.14. Available at `https://arxiv.org/abs/1904.04735`.

[37] Aleks Kissinger & John van de Wetering (2020): *Reducing the number of non-Clifford gates in quantum circuits*. *Phys. Rev. A* 102, p. 022406, doi:10.1103/PhysRevA.102.022406. Available at `https://link.aps.org/doi/10.1103/PhysRevA.102.022406`.

[38] Aleks Kissinger & Vladimir Zamdzhiev (2015): *Quantomatic: A proof assistant for diagrammatic reasoning*. In: *International Conference on Automated Deduction*, Springer, pp. 326–336. Available at `http://quantomatic.github.io/`.

[39] Jarrod R McClean, Sergio Boixo, Vadim N Smelyanskiy, Ryan Babbush & Hartmut Neven (2018): *Barren plateaus in quantum neural network training landscapes*. *Nature communications* 9(1), pp. 1–6.

[40] Jarrod R McClean, Jonathan Romero, Ryan Babbush & Alán Aspuru-Guzik (2016): *The theory of variational hybrid quantum-classical algorithms*. *New Journal of Physics* 18(2), p. 023023.

[41] Alberto Peruzzo, Jarrod McClean, Peter Shadbolt, Man-Hong Yung, Xiao-Qi Zhou, Peter J Love, Alán Aspuru-Guzik & Jeremy L O'brien (2014): *A variational eigenvalue solver on a photonic quantum processor*. *Nature communications* 5(1), pp. 1–7, doi:10.1038/ncomms5213.

[42] John Preskill (2018): *Quantum computing in the NISQ era and beyond*. *Quantum* 2, p. 79.

[43] André Ranchin (2014): *Depicting qudit quantum mechanics and mutually unbiased qudit theories*. In Bob Coecke, Ichiro Hasuo & Prakash Panangaden, editors: Proceedings of the 11th workshop on *Quantum Physics and Logic*, Kyoto, Japan, 4-6th June 2014, *Electronic Proceedings in Theoretical Computer Science* 172, Open Publishing Association, pp. 68–91, doi:10.4204/EPTCS.172.6. Available at `https://arxiv.org/abs/1404.1288`.

[44] Ruslan Shaydulin, Stuart Hadfield, Tad Hogg & Ilya Safro (2021): *Classical symmetries and the Quantum Approximate Optimization Algorithm*. *Quantum Information Processing* 20(11), pp. 1–28.

[45] Ruslan Shaydulin & Stefan M Wild (2021): *Exploiting symmetry reduces the cost of training QAOA*. *IEEE Transactions on Quantum Engineering* 2, pp. 1–9.

[46] Tobias Stollenwerk, Stuart Hadfield & Zhihui Wang (2020): *Toward Quantum Gate-Model Heuristics for Real-World Planning Problems*. *IEEE Transactions on Quantum Engineering* 1, pp. 1–16, doi:10.1109/TQE.2020.3030609.

[47] Michael Streif & Martin Leib (2020): *Training the quantum approximate optimization algorithm without access to a quantum processing unit*. *Quantum Science and Technology* 5(3), p. 034008.

[48] Alexis Toumi, Richie Yeung & Giovanni de Felice (2021): *Diagrammatic Differentiation for Quantum Machine Learning*. In Chris Heunen & Miriam Backens, editors: Proceedings 18th International Conference on *Quantum Physics and Logic*, Gdansk, Poland, and online, 7-11 June 2021, *Electronic Proceedings in Theoretical Computer Science* 343, Open Publishing Association, pp. 132–144, doi:10.4204/EPTCS.343.7. Available at `https://arxiv.org/abs/2103.07960`.

[49] Alex Townsend-Teague & Konstantinos Meichanetzidis (2021): *Classifying Complexity with the ZX-Calculus: Jones Polynomials and Potts Partition Functions*. *arXiv preprint arXiv:2103.06914*. Available at `https://arxiv.org/abs/2103.06914`.

[50] Renaud Vilmart (2019): *A near-minimal axiomatisation of ZX-calculus for pure qubit quantum mechanics*. In: *2019 34th Annual ACM/IEEE Symposium on Logic in Computer Science (LICS)*, IEEE, pp. 1–10.

[51] Quanlong Wang & Xiaoning Bian (2014): *Qutrit Dichromatic Calculus and Its Universality*. In Bob Coecke, Ichiro Hasuo & Prakash Panangaden, editors: Proceedings of the 11th workshop on *Quantum Physics and Logic*, Kyoto, Japan, 4-6th June 2014, *Electronic Proceedings in Theoretical Computer Science* 172, Open Publishing Association, pp. 92–101, doi:10.4204/EPTCS.172.7. Available at `https://arxiv.org/abs/1406.3056`.

[52] Quanlong Wang & Richie Yeung (2022): *Differentiating and Integrating ZX Diagrams*. arXiv preprint arXiv:2201.13250. Available at https://arxiv.org/abs/2201.13250.

[53] Zhihui Wang, Stuart Hadfield, Zhang Jiang & Eleanor G Rieffel (2018): *Quantum approximate optimization algorithm for MaxCut: A fermionic view*. Physical Review A 97(2), p. 022304.

[54] Zhihui Wang, Nicholas C. Rubin, Jason M. Dominy & Eleanor G. Rieffel (2020): *XY mixers: Analytical and numerical results for the quantum alternating operator ansatz*. Phys. Rev. A 101, p. 012320, doi:10.1103/PhysRevA.101.012320. Available at https://link.aps.org/doi/10.1103/PhysRevA.101.012320.

[55] John van de Wetering (2020): *ZX-calculus for the working quantum computer scientist*. arXiv preprint arXiv:2012.13966. Available at https://arxiv.org/abs/2012.13966.

[56] David Wierichs, Josh Izaac, Cody Wang & Cedric Yen-Yu Lin (2022): *General parameter-shift rules for quantum gradients*. Quantum 6, p. 677, doi:10.22331/q-2022-03-30-677. Available at https://doi.org/10.22331/q-2022-03-30-677.

[57] Richie Yeung (2020): *Diagrammatic Design and Study of Ansätze for Quantum Machine Learning*. arXiv preprint arXiv:2011.11073. Available at https://arxiv.org/abs/2011.11073.

[58] Chen Zhao & Xiao-Shan Gao (2021): *Analyzing the barren plateau phenomenon in training quantum neural networks with the ZX-calculus*. Quantum 5, p. 466. Available at https://doi.org/10.22331/q-2021-06-04-466.

A Additional Rules for Linear Combinations of ZX-Diagrams

We introduce several additional rules which are useful for the calculation of expectation values for PQC which we utilize in the derivations to follow.

Scalar-pull rule First, scalars can be pulled through the bubble. I.e. it does not matter if we write them to the left or right of the bubbles.

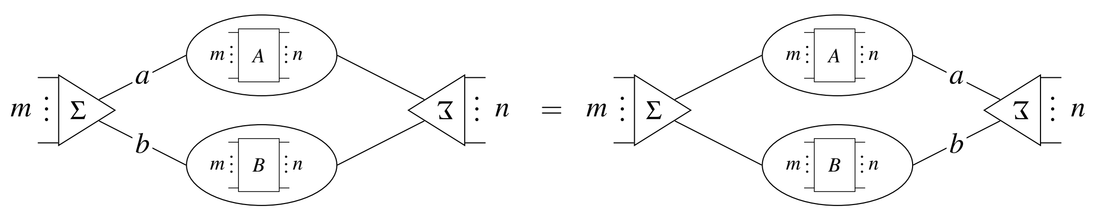

Linear combinations for states and effects Since we can put the scalar factor left or right of the bubbles, we can simplify linear combinations in the case of states or effects. For states (no inputs), we can cut the left half of the diagram

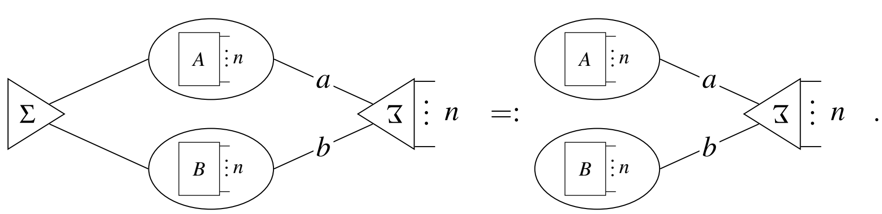

For effects (no outputs), we can cut the right half of the diagram

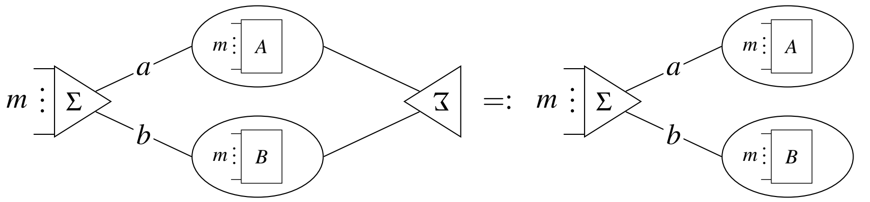

Direct connection of diagrams (no bubbles) We can also completely drop the bubbles and continue the input and output wires through the sum symbols

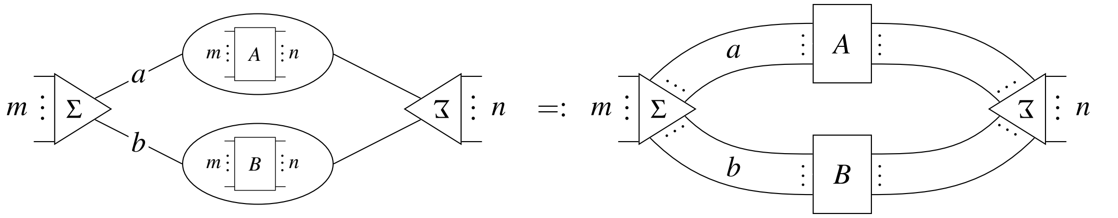

However, we will not require this notation in the examples considered in this paper.

B Additional Examples

Here we continue our examples from Section 4 and diagrammatically derive MaxCut expectation values for a hardware efficient ansatz as well as for QAOA_1 on rings and general graphs.

B.1 Hardware Efficient Ansatz

We consider a variant of a hardware efficient SU-2 2-local ansatz from Qiskit [2]. This ansatz was also studied in [24]. For simplicity here we consider a 3-qubit realization,

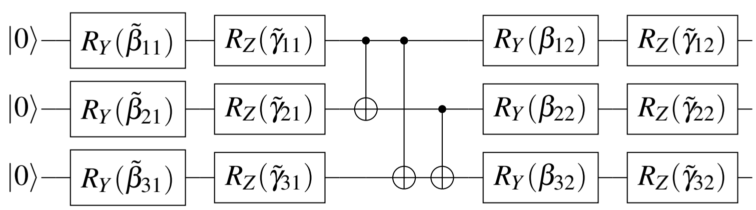

$$= \frac{1}{\sqrt{2^3}}$$

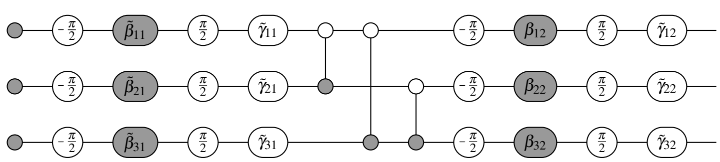

$$\overset{(f),(c)}{=} \frac{1}{\sqrt{2^3}}$$

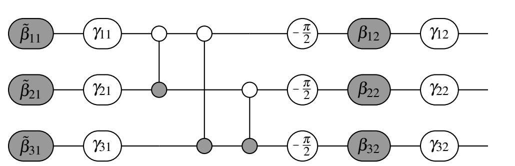

,

where we conveniently set $\gamma_{ij} := \tilde{\gamma}_{ij} + \frac{\pi}{2}$ and $\beta_{ij} := \frac{-\tilde{\beta}ij}{2}$. To compute the expectation value of a given cost Hamiltonian, we again requite expectation values of products of Pauli-Z operators. We demonstrate how such calculations can be performed diagrammatically by considering again MaxCut as an example. For the expectation value corresponding to a given edge $(2,3)$ we have

$\langle Z_2 Z_3 \rangle =$

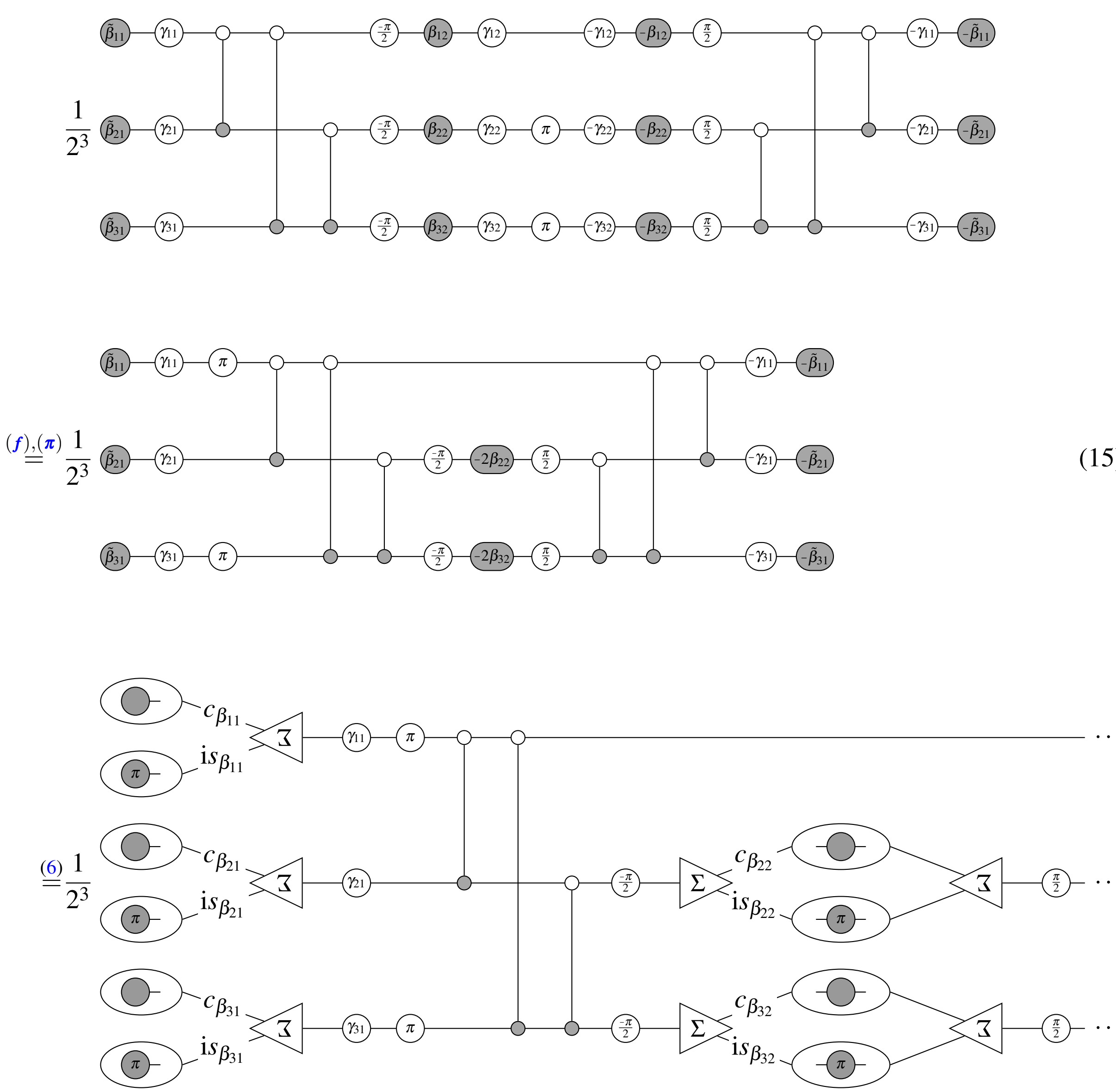

(15)

$$\overset{(f),(i)}{=} \frac{1}{2^3}$$

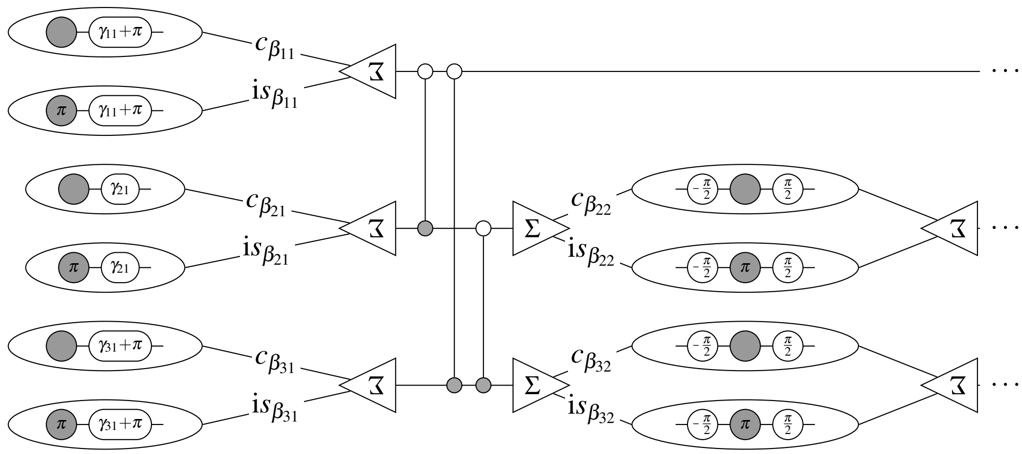

$$\overset{(c)\,(\pi)\,(f)}{=} \frac{1}{2^3}$$

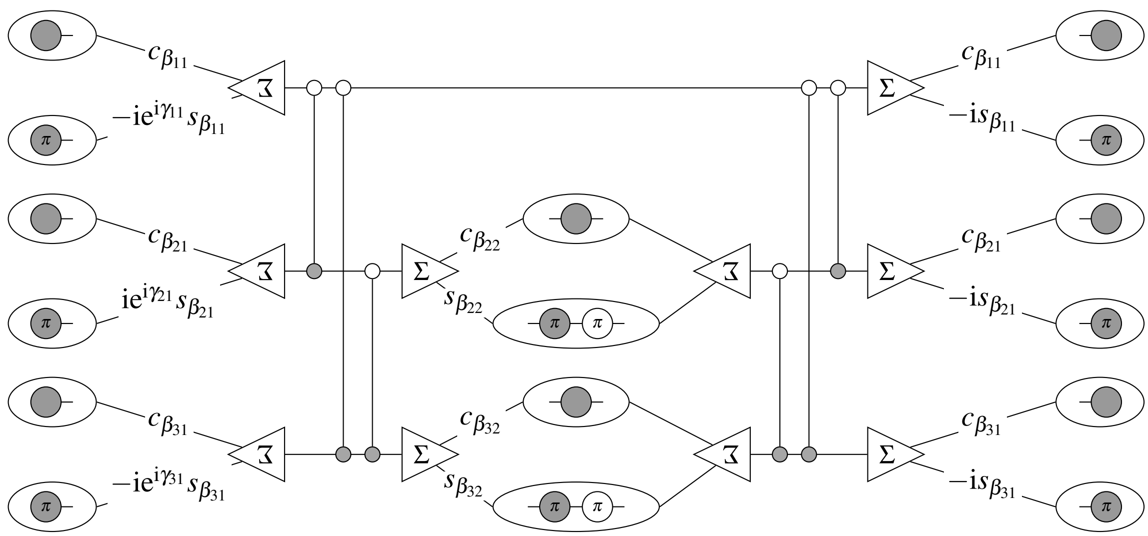

$$\begin{aligned}
&\overset{(17)}{=} c_{\beta_{11}}^2 c_{\beta_{21}}^2 c_{\beta_{22}} c_{\beta_{31}}^2 c_{\beta_{32}} - \mathrm{i}c_{\beta_{11}}^2 c_{\beta_{21}}^2 c_{\beta_{22}} c_{\beta_{31}} s_{\beta_{31}} s_{\beta_{32}} e^{\mathrm{i}\gamma_{31}} \\
&\quad + \mathrm{i}c_{\beta_{11}}^2 c_{\beta_{21}}^2 c_{\beta_{22}} c_{\beta_{31}} s_{\beta_{31}} s_{\beta_{32}} - c_{\beta_{11}}^2 c_{\beta_{21}}^2 c_{\beta_{22}} c_{\beta_{32}} s_{\beta_{31}}^2 e^{\mathrm{i}\gamma_{31}} \\
&\quad + \mathrm{i}c_{\beta_{11}}^2 c_{\beta_{21}} c_{\beta_{31}}^2 s_{\beta_{21}} s_{\beta_{22}} s_{\beta_{32}} e^{\mathrm{i}\gamma_{21}} - \mathrm{i}c_{\beta_{11}}^2 c_{\beta_{21}} c_{\beta_{31}}^2 s_{\beta_{21}} s_{\beta_{22}} s_{\beta_{32}} \\
&\quad + c_{\beta_{11}}^2 c_{\beta_{21}} c_{\beta_{31}} c_{\beta_{32}} s_{\beta_{21}} s_{\beta_{22}} s_{\beta_{31}} e^{\mathrm{i}\gamma_{21}} e^{\mathrm{i}\gamma_{31}} + c_{\beta_{11}}^2 c_{\beta_{21}} c_{\beta_{31}} c_{\beta_{32}} s_{\beta_{21}} s_{\beta_{22}} s_{\beta_{31}} e^{\mathrm{i}\gamma_{21}} \\
&\quad + c_{\beta_{11}}^2 c_{\beta_{21}} c_{\beta_{31}} c_{\beta_{32}} s_{\beta_{21}} s_{\beta_{22}} s_{\beta_{31}} e^{\mathrm{i}\gamma_{31}} + c_{\beta_{11}}^2 c_{\beta_{21}} c_{\beta_{31}} c_{\beta_{32}} s_{\beta_{21}} s_{\beta_{22}} s_{\beta_{31}} \\
&\quad + \mathrm{i}c_{\beta_{11}}^2 c_{\beta_{21}} s_{\beta_{21}} s_{\beta_{22}} s_{\beta_{31}}^2 s_{\beta_{32}} e^{\mathrm{i}\gamma_{21}} e^{\mathrm{i}\gamma_{31}} - \mathrm{i}c_{\beta_{11}}^2 c_{\beta_{21}} s_{\beta_{21}} s_{\beta_{22}} s_{\beta_{31}}^2 s_{\beta_{32}} e^{\mathrm{i}\gamma_{31}} \\
&\quad + c_{\beta_{11}}^2 c_{\beta_{22}} c_{\beta_{31}}^2 c_{\beta_{32}} s_{\beta_{21}}^2 e^{\mathrm{i}\gamma_{21}} + \mathrm{i}c_{\beta_{11}}^2 c_{\beta_{22}} c_{\beta_{31}} s_{\beta_{21}}^2 s_{\beta_{31}} s_{\beta_{32}} e^{\mathrm{i}\gamma_{21}} e^{\mathrm{i}\gamma_{31}} \\
&\quad - \mathrm{i}c_{\beta_{11}}^2 c_{\beta_{22}} c_{\beta_{31}} s_{\beta_{21}}^2 s_{\beta_{31}} s_{\beta_{32}} e^{\mathrm{i}\gamma_{21}} - c_{\beta_{11}}^2 c_{\beta_{22}} c_{\beta_{32}} s_{\beta_{21}}^2 s_{\beta_{31}}^2 e^{\mathrm{i}\gamma_{21}} e^{\mathrm{i}\gamma_{31}} \\
&\quad - c_{\beta_{21}}^2 c_{\beta_{22}} c_{\beta_{31}}^2 s_{\beta_{11}}^2 s_{\beta_{32}} e^{\mathrm{i}\gamma_{11}} + \mathrm{i}c_{\beta_{21}}^2 c_{\beta_{22}} c_{\beta_{31}} c_{\beta_{32}} s_{\beta_{11}}^2 s_{\beta_{31}} e^{\mathrm{i}\gamma_{11}} e^{\mathrm{i}\gamma_{31}} \\
&\quad + \mathrm{i}c_{\beta_{21}}^2 c_{\beta_{22}} c_{\beta_{31}} c_{\beta_{32}} s_{\beta_{11}}^2 s_{\beta_{31}} e^{\mathrm{i}\gamma_{11}} - c_{\beta_{21}}^2 c_{\beta_{22}} s_{\beta_{11}}^2 s_{\beta_{31}}^2 s_{\beta_{32}} e^{\mathrm{i}\gamma_{11}} e^{\mathrm{i}\gamma_{31}}
\end{aligned}$$

$$
\begin{aligned}
&+\mathrm{i}c_{\beta_{21}}c^2_{\beta_{31}}c_{\beta_{32}}s^2_{\beta_{11}}s_{\beta_{21}}s_{\beta_{22}}\mathrm{e}^{\mathrm{i}\gamma_{11}}\mathrm{e}^{\mathrm{i}\gamma_{21}}+\mathrm{i}c_{\beta_{21}}c^2_{\beta_{31}}c_{\beta_{32}}s^2_{\beta_{11}}s_{\beta_{21}}s_{\beta_{22}}\mathrm{e}^{\mathrm{i}\gamma_{11}}\\
&+c_{\beta_{21}}c_{\beta_{31}}s^2_{\beta_{11}}s_{\beta_{21}}s_{\beta_{22}}s_{\beta_{31}}s_{\beta_{32}}\mathrm{e}^{\mathrm{i}\gamma_{11}}\mathrm{e}^{\mathrm{i}\gamma_{21}}\mathrm{e}^{\mathrm{i}\gamma_{31}}-c_{\beta_{21}}c_{\beta_{31}}s^2_{\beta_{11}}s_{\beta_{21}}s_{\beta_{22}}s_{\beta_{31}}s_{\beta_{32}}\mathrm{e}^{\mathrm{i}\gamma_{11}}\mathrm{e}^{\mathrm{i}\gamma_{21}}\\
&-c_{\beta_{21}}c_{\beta_{31}}s^2_{\beta_{11}}s_{\beta_{21}}s_{\beta_{22}}s_{\beta_{31}}s_{\beta_{32}}\mathrm{e}^{\mathrm{i}\gamma_{11}}\mathrm{e}^{\mathrm{i}\gamma_{31}}+c_{\beta_{21}}c_{\beta_{31}}s^2_{\beta_{11}}s_{\beta_{21}}s_{\beta_{22}}s_{\beta_{31}}s_{\beta_{32}}\mathrm{e}^{\mathrm{i}\gamma_{11}}\\
&-\mathrm{i}c_{\beta_{21}}c_{\beta_{32}}s^2_{\beta_{11}}s_{\beta_{21}}s_{\beta_{22}}s^2_{\beta_{31}}\mathrm{e}^{\mathrm{i}\gamma_{11}}\mathrm{e}^{\mathrm{i}\gamma_{21}}\mathrm{e}^{\mathrm{i}\gamma_{31}}-\mathrm{i}c_{\beta_{21}}c_{\beta_{32}}s^2_{\beta_{11}}s_{\beta_{21}}s_{\beta_{22}}s^2_{\beta_{31}}\mathrm{e}^{\mathrm{i}\gamma_{11}}\mathrm{e}^{\mathrm{i}\gamma_{31}}\\
&+c_{\beta_{22}}c^2_{\beta_{31}}s^2_{\beta_{11}}s^2_{\beta_{21}}s_{\beta_{32}}\mathrm{e}^{\mathrm{i}\gamma_{11}}\mathrm{e}^{\mathrm{i}\gamma_{21}}+\mathrm{i}c_{\beta_{22}}c_{\beta_{31}}c_{\beta_{32}}s^2_{\beta_{11}}s^2_{\beta_{21}}s_{\beta_{31}}\mathrm{e}^{\mathrm{i}\gamma_{11}}\mathrm{e}^{\mathrm{i}\gamma_{21}}\mathrm{e}^{\mathrm{i}\gamma_{31}}\\
&+\mathrm{i}c_{\beta_{22}}c_{\beta_{31}}c_{\beta_{32}}s^2_{\beta_{11}}s^2_{\beta_{21}}s_{\beta_{31}}\mathrm{e}^{\mathrm{i}\gamma_{11}}\mathrm{e}^{\mathrm{i}\gamma_{21}}+c_{\beta_{22}}s^2_{\beta_{11}}s^2_{\beta_{21}}s^2_{\beta_{31}}s_{\beta_{32}}\mathrm{e}^{\mathrm{i}\gamma_{11}}\mathrm{e}^{\mathrm{i}\gamma_{21}}\mathrm{e}^{\mathrm{i}\gamma_{31}}\,,
\end{aligned}
\tag{16}
$$

where in the last step we have used the identity

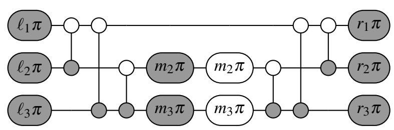

$$= \frac{f^{r_1r_2r_3}_{m_2m_3}}{2^3}$$

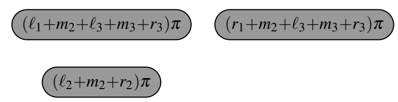

$$
= \begin{cases} 0 & \text{if} \quad \begin{array}{l} \ell_1+m_2+\ell_3+m_3+r_3 \text{ odd} \\ \vee\, r_1+m_2+\ell_3+m_3+r_3 \text{ odd} \\ \vee\, \ell_2+m_2+r_2 \text{ odd} \end{array} \\ f^{r_1r_2r_3}_{m_2m_3} & \text{else} \end{cases}\,, \tag{17}
$$

with $\ell_1,\ell_2,\ell_3,m_2,m_3,r_1,r_2,r_3\in\{0,1\}^{\times 8}$ and $f^{r_1r_2r_3}_{m_2m_3} := (-1)^{m_2r_1+(m_2\oplus m_3)r_2+m_3r_3}$, which is the proven in Appendix D.2. Observe that in the second step above any dependency on the parameters γ_{12},γ_{22}, and γ_{32} was immediately shown to cancel out (due to commuting with the diagonal cost Hamiltonian), and likewise for β_{12} (due to the locality of Z_2Z_3). Similar simplifications are often easily obtained from the diagrammatic perspective.

The formula (16) exemplifies the significant difficulty faced in obtaining analytical results for PQCs, even for relatively small ansätze. Nevertheless, in our analysis the complexity remained manageable with the diagrammatic approach up until the very last step, were we applied a simple numerical procedure to collect all the surviving terms (according to (17)) of the contraction. Different hardware-efficient ansätze may be similarly considered, including ones tailored to specific hardware topology. As mentioned, for deeper or more complicated ansätze, analysis may be aided or automated through implementation in software. Here (15) demonstrates how diagrammatic approaches can yield more compact representations of expectation values (as compared to (16)).

B.2 QAOA for MaxCut on Ring graphs

We consider the simple example of the one-dimensional "ring-of-disagrees", i.e., 2-regular connected graphs, and rederive the QAOA$_1$ expectation value as previously shown in [22, 53]. First consider the case of QAOA with arbitrary number of layers p, with $n \gg p$. From the problem symmetry, it suffices to consider the expectation value of a single edge term $\langle Z_iZ_{i+1}\rangle_{QAOA_p}$. Applying the lightcone rule (9), the outermost reduced phase-separation layer (10) reads

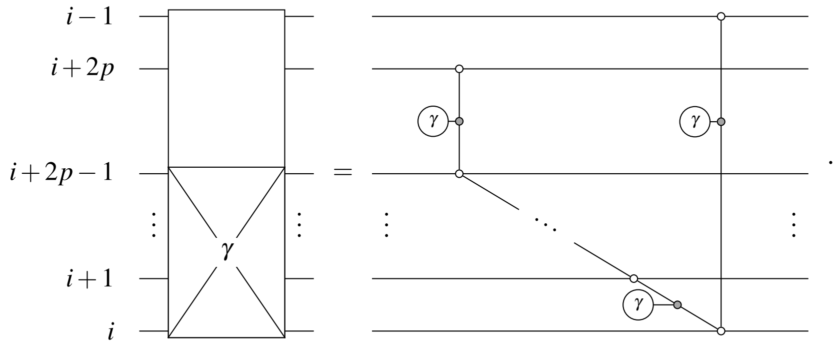

Hence for the QAOA$_p$ expectation value we obtain

$\langle Z_i Z_{i+1} \rangle_{\mathrm{QAOA}_p}$

$$= \frac{1}{2^{2(p+1)}}$$

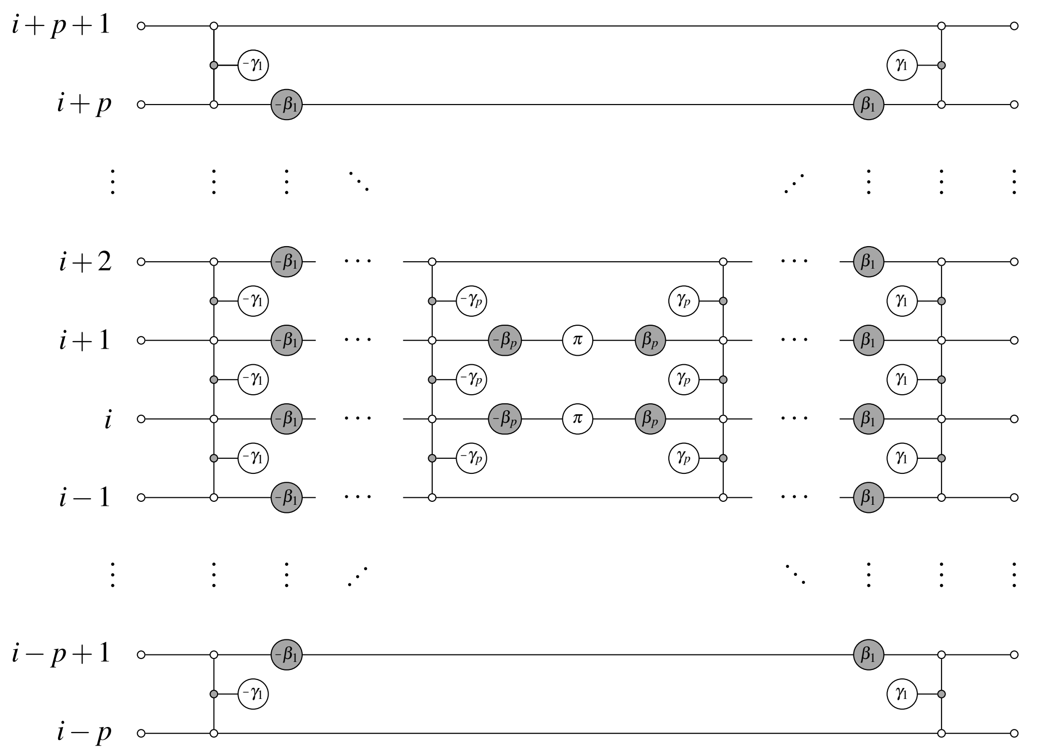

Observe how the problem and structure again appears in the above diagram (i.e., p-neighborhoods of the edge $(i,i+1)$ are line graphs). Furthermore, the utility of the lightcone rule is clearly demonstrated here.

Continuing for the $p = 1$ case, we get

$$\langle Z_i Z_{i+1} \rangle_{\mathrm{QAOA}_1} = \frac{2^3}{2^4}$$

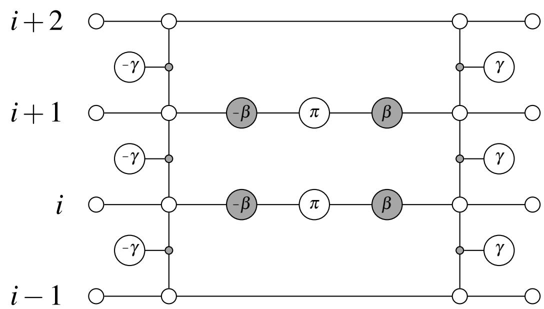

$$\overset{(\pi),(f)}{=} \frac{\mathrm{e}^{-2\mathrm{i}\beta}}{2}$$

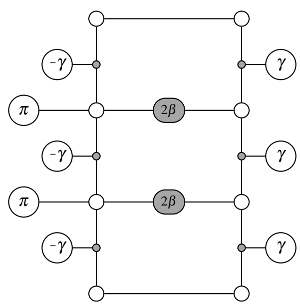

$$\overset{(6)}{=} \frac{1}{2}$$

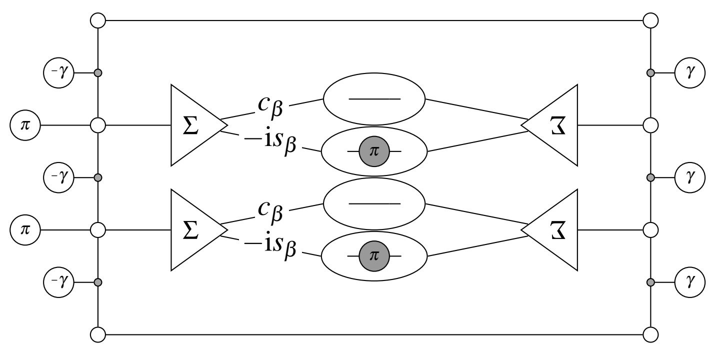

$$\overset{(\mathrm{i}),(\mathrm{ii})}{=} \frac{1}{2}$$

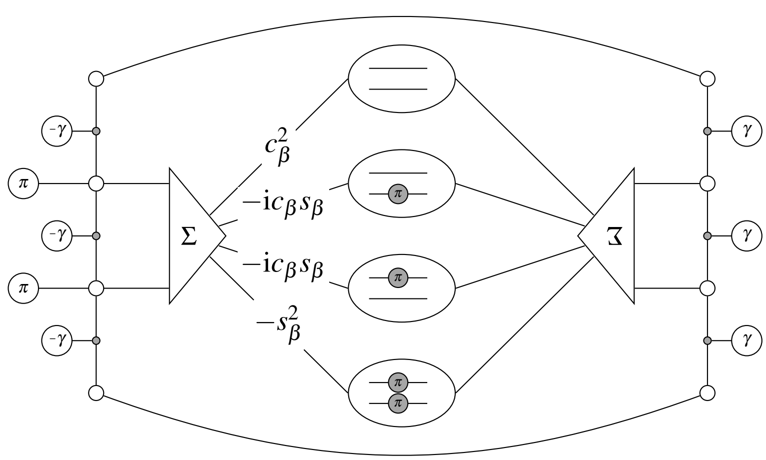

$$\overset{(i)}{=} \frac{1}{2}$$

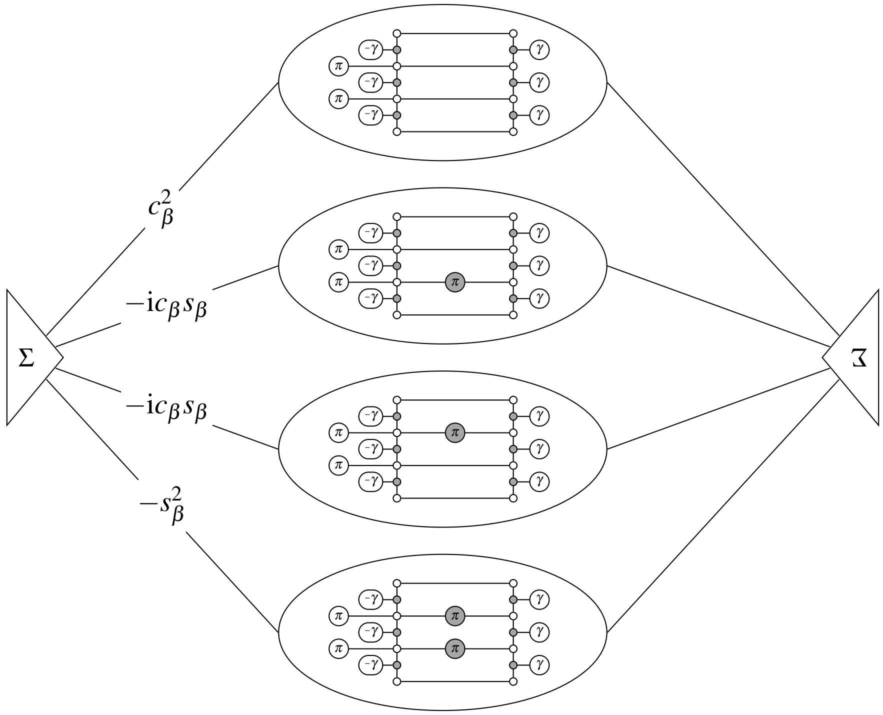

$$\overset{(8)}{=} \frac{1}{2}$$

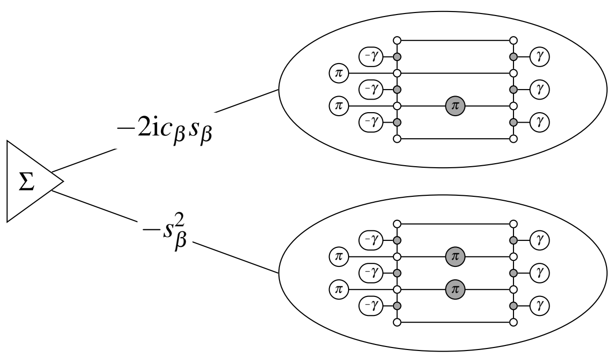

$$\overset{(\pi)}{\underset{}{\overset{(8)}{=}}} \frac{\mathrm{e}^{2\mathrm{i}\gamma}}{2^3}$$

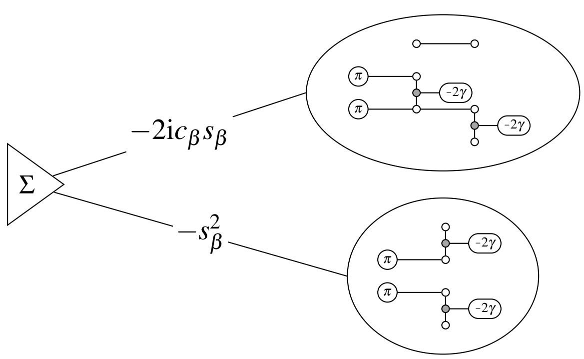

$$\overset{(7)}{=} -2\mathrm{i}c_\beta s_\beta \frac{\mathrm{e}^{2\mathrm{i}\gamma}}{2^3}$$

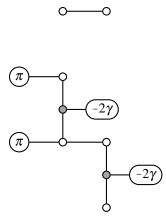

$$\overset{(7)}{=} \frac{-2\mathrm{i}c_\beta s_\beta}{2^4}$$

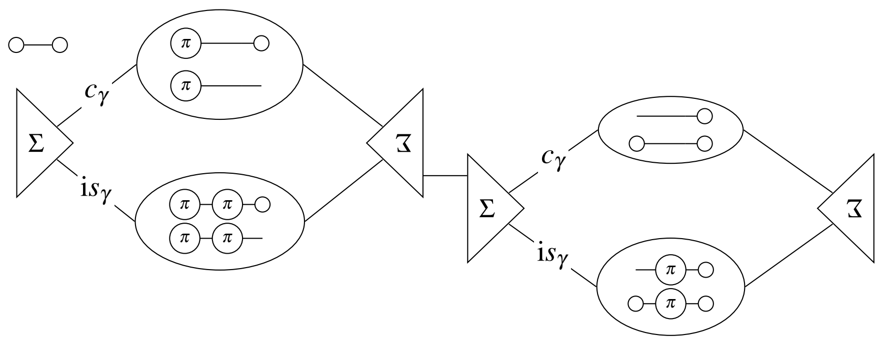

$$= 2c_\beta s_\beta s_\gamma c_\gamma$$

The result is consistent with that of [53, Thm. 1]. The expression obtained for $\langle C\rangle$ is easily optimized to reproduce the performance result obtained numerically for the ring of disagrees in [22]. Similar to the previous examples, here we saw the necessity of our extension for handling X-Z commutations in the third and seventh steps of the derivation above.

In Appendix B.3 we show the same calculation for MaxCut on general graphs, as obtained for QAOA$_1$ in [53, Thm. 1]. Similar techniques may be applied and results obtained for a wide variety of important problems, for instance quadratic binary optimization problems of which MaxCut is a special case.

B.3 QAOA$_1$ for MaxCut on General Graphs

For the QAOA expectation value for MaxCut $\langle C\rangle = \frac{|E|}{2} - \frac{1}{2}\sum_{u,v\in E}\langle Z_u Z_v\rangle$ on general graphs we need to calculate the contributions $\langle Z_u Z_v\rangle$. In this section, we perform the calculation for general graphs in the QAOA, $p = 1$ case, reproducing results obtained in [53].

Following the lightcone rule from Equation (9) we obtain for Z-Z terms in the MaxCut QAOA$_1$ expectation value on a general graph $G = (V, E)$

$$\langle Z_u Z_v\rangle_{\mathrm{QAOA}_1} \overset{(9)}{=} \frac{1}{2^{|V|}}$$

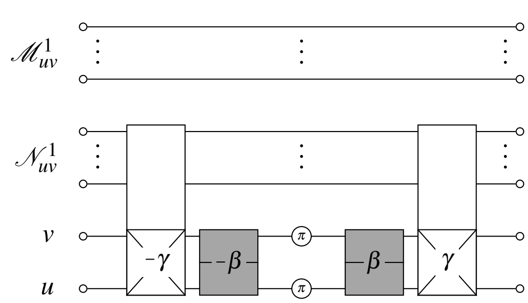

$$\overset{(11)}{\underset{(\boldsymbol{\pi})}{=}} \frac{\mathrm{e}^{-2\mathrm{i}\beta}}{2^{|\mathcal{N}_{uv}^{1}|+2}}$$

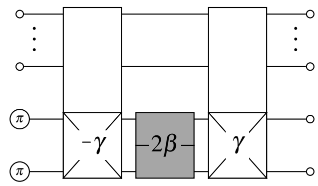

$$\overset{(6)}{\underset{(\mathrm{ii})}{=}} \frac{1}{2^{|\mathcal{N}_{uv}^{1}|+2}}$$

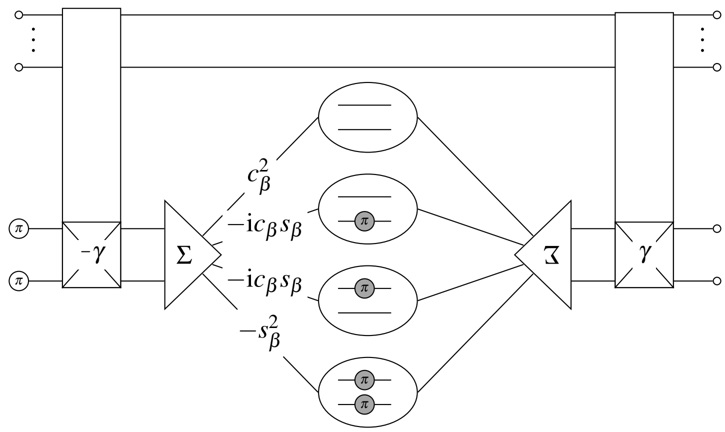

$$\overset{(\mathrm{i})}{=} \frac{1}{2^{|\mathcal{N}_{uv}^{1}|+2}}$$

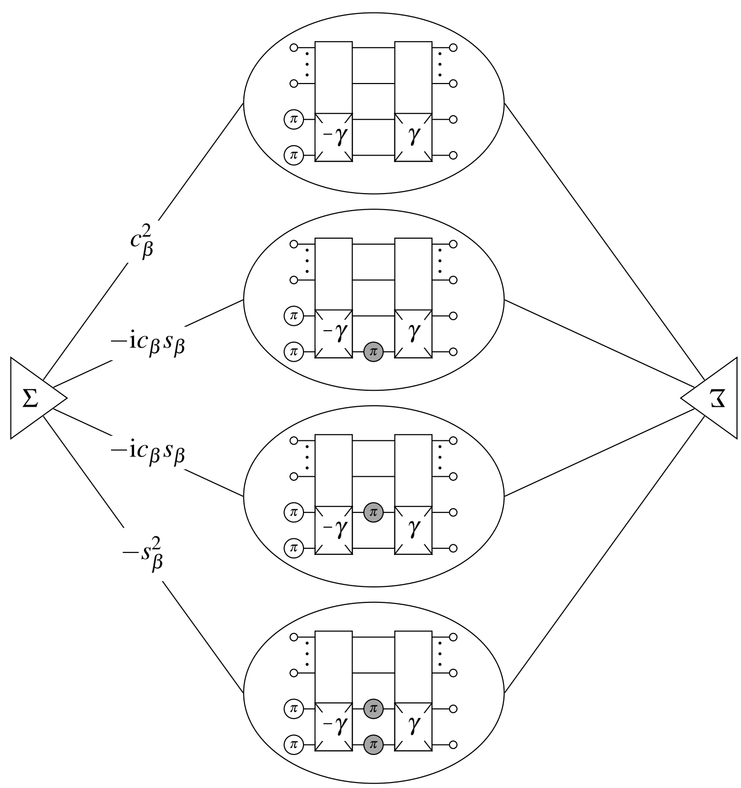

.

The first summand vanishes and the second and third are linked by symmetry. We continue with the second summand (the *I*-*X*-term)

$$\frac{1}{2^{|\mathcal{N}_{uv}^1|+2}}$$

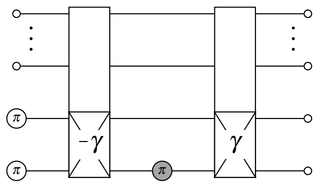

$$\overset{(10)}{=} \frac{2^{n_u+2n_{uv}+n_v+1}}{2^{|\mathcal{N}_{uv}^1|+2}}$$

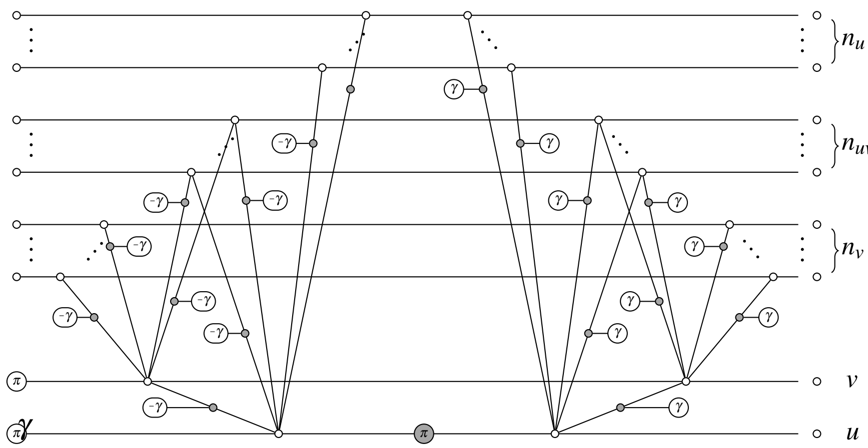

$$\overset{(\pi)(c)(8)}{=} \frac{2^{n_u+n_{uv}+1}}{2^{|\mathcal{N}_{uv}^1|+2}}$$

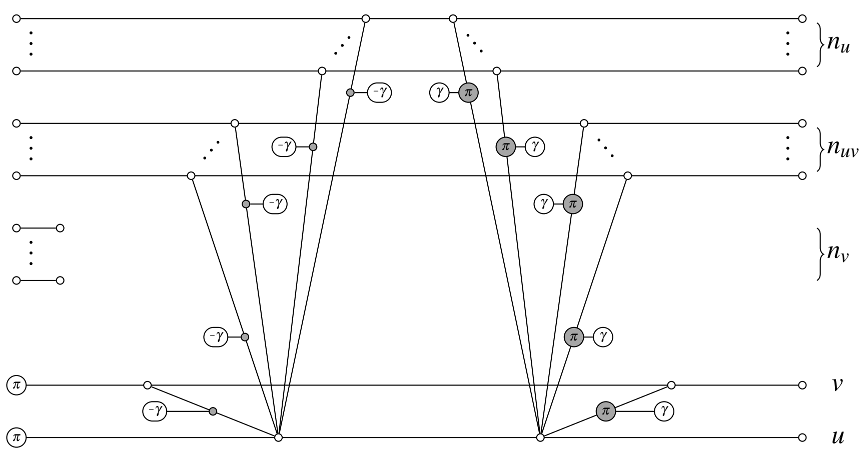

$$\overset{(f)}{=} \frac{2^{n_u+n_{uv}+n_v+1}}{2^{|\mathcal{N}_{uv}^1|+2}}$$

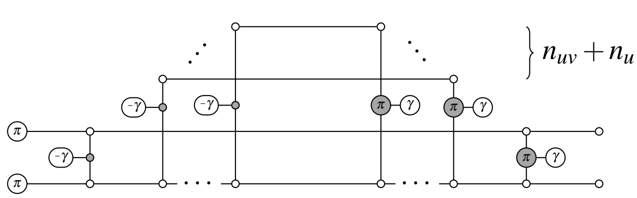

$$\overset{(f)(18)}{=} \frac{c_\gamma^{n_u+n_{uv}}}{2}$$

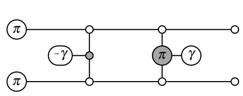

$$\overset{(8)}{\underset{(7)}{=}} \frac{c_\gamma^{n_u+n_{uv}}}{2^2}$$

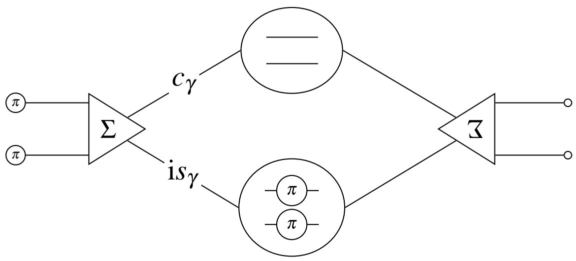

$$= \mathrm{i} s_\gamma c_\gamma^{n_u+n_{uv}} \, ,$$

where we have used the size of the exclusive neighborhoods $n_u := |N_u \setminus \{N_v \cup u\}|$, $n_v := |N_v \setminus \{N_u \cup v\}|$, and the joined neighborhood $n_{uv} := |N_u \cap N_v|$, the relation $|\mathcal{N}^1_{uv}| = n_u + n_{uv} + n_v$, as well as

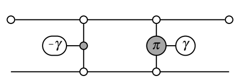

$$\overset{(8)}{=} \frac{\mathrm{e}^{\mathrm{i}\gamma}}{\sqrt{2}}$$

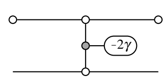

$$\overset{(7)}{=} \frac{1}{2}$$

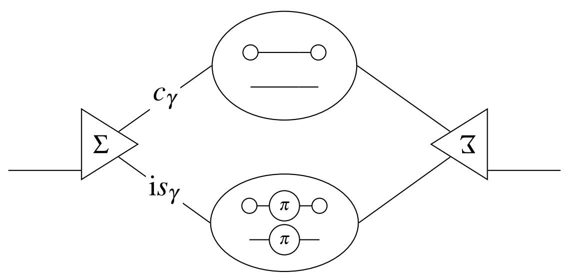

$$= c_\gamma \quad . \tag{18}$$

Analogously the third summand (the X-I-term) can be obtained as

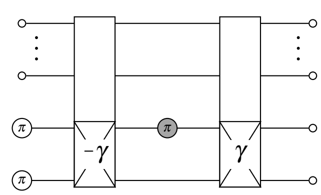

$$= \mathrm{i} s_\gamma c_\gamma^{n_v+n_{uv}} \, .$$

The fourth summand (the X-X-term) reads

$$\frac{1}{2^{|\mathcal{N}^1_{uv}|+2}}$$

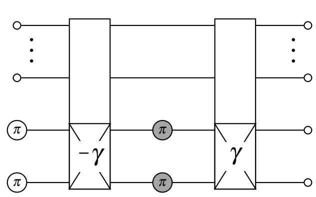

$$\overset{(10)}{=} \frac{2^{n_u+2n_{uv}+n_v+1}}{2^{|\mathcal{N}_{uv}^1|+2}}$$

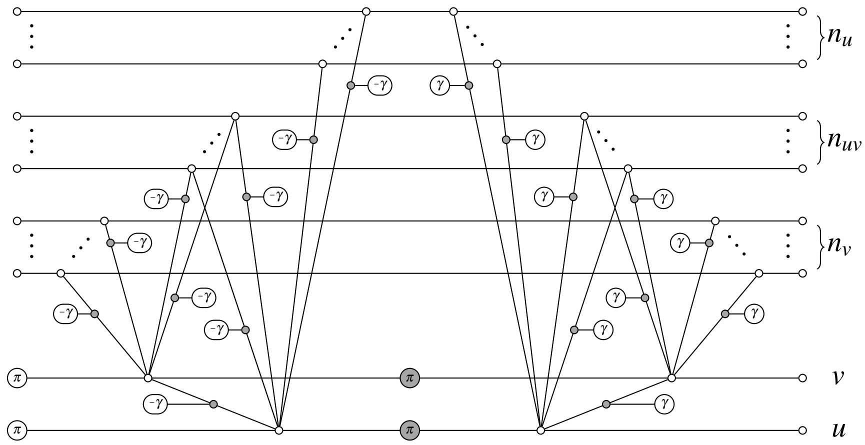

$$\overset{(\pi)}{\underset{(8)}{=}} \frac{2^{n_u+2n_{uv}+n_v}}{2^{|\mathcal{N}_{uv}^1|+2}}$$

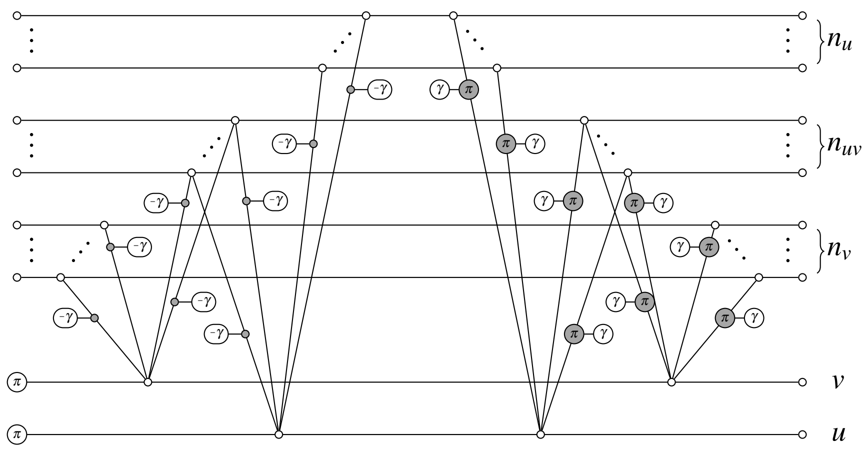

$$\overset{(f)}{\underset{(7)}{=}} \frac{2^{n_{uv}}}{2^2}\left(\frac{e^{i\gamma}}{\sqrt{2}}\right)^{n_u+2n_{uv}+n_v}$$

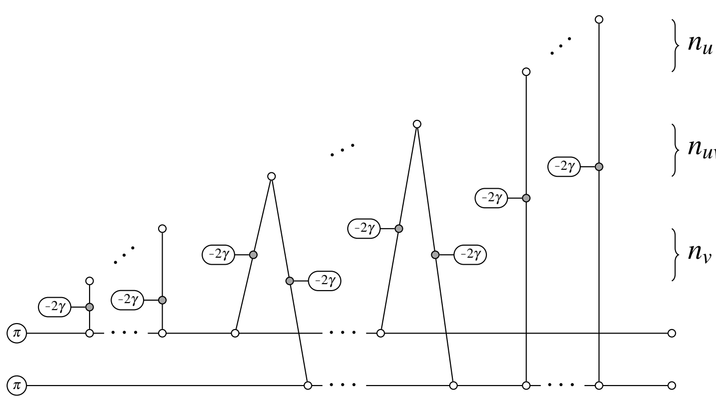

$$\overset{(18)(19)}{=} \frac{c_\gamma^{n_u+n_v}}{2^2}$$

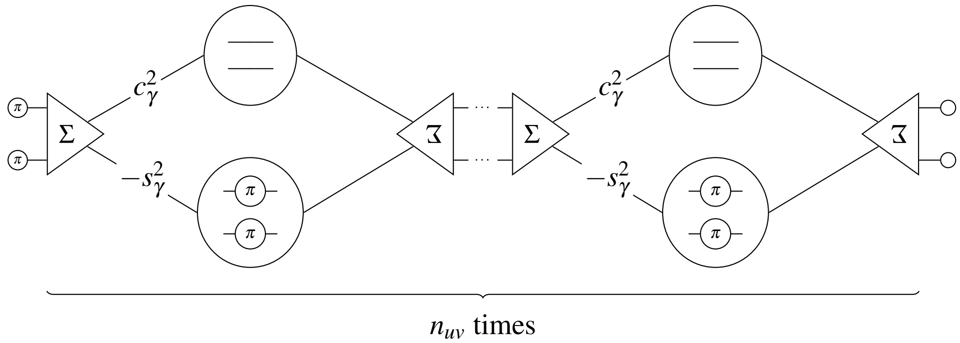

$$\overset{(ii)}{=} \frac{-c_\gamma^{n_u+n_v}}{2^2} \Bigg\{ \binom{n_{uv}}{1} s_\gamma^2 c_\gamma^{n_{uv}-2}$$

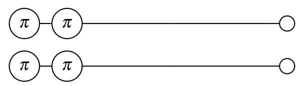

$$+ \binom{n_{uv}}{3} s_\gamma^6 c_\gamma^{n_{uv}-6}$$

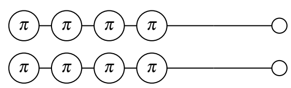

$$+ \binom{n_{uv}}{5} s_\gamma^{10} c_\gamma^{n_{uv}-10}$$

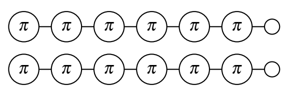

$$+ \dots \Bigg\}$$

$$= -c_\gamma^{n_u+n_v} \sum_{i=1,3,\dots} \binom{n_{uv}}{i} (s_\gamma^2)^i (c_\gamma^2)^{n_{uv}-i},$$

where we have used

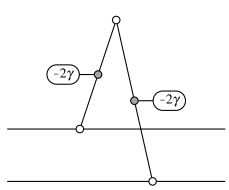

$$\overset{(f)}{=}$$

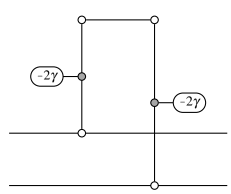

$$\overset{(7)}{=} \left(\frac{e^{-i\gamma}}{\sqrt{2}}\right)^2$$

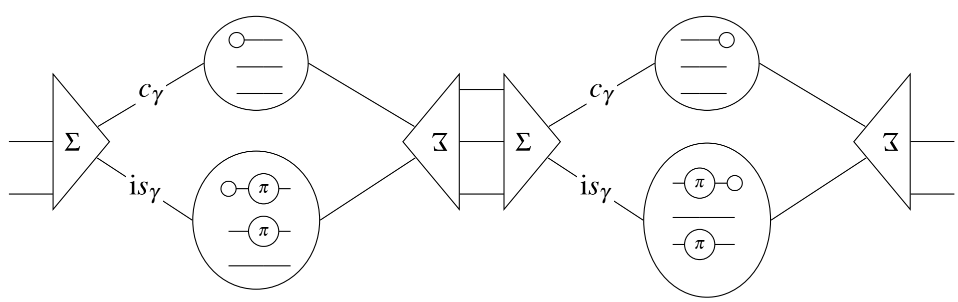

$$=2\left(\frac{\mathrm{e}^{-\mathrm{i}\gamma}}{\sqrt{2}}\right)^2$$

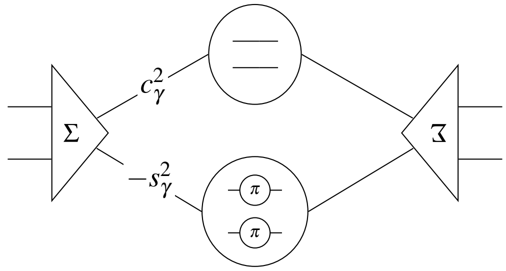

$$. \qquad (19)$$

Hence, the total Z-Z-expectation value reads

$$\langle Z_u Z_v\rangle_{\mathrm{QAOA}_1} = c_\beta s_\beta s_\gamma \left(c_\gamma^{n_u+n_{uv}} + c_\gamma^{n_v+n_{uv}}\right) + c_\gamma^{n_u+n_v} s_\beta^2 \sum_{i=1,3,\ldots} \binom{n_{uv}}{i} (s_\gamma^2)^i (c_\gamma^2)^{n_{uv}-i}.$$

This result is consistent with the corresponding QAOA_1 performance analysis of [53]; applying the binomial theorem to write the sum above in closed form then leads directly to the result of [53, Thm. 1].

C Details on QAOA_1 for MaxCut on Simple Graph

We calculate each of the four summands in (14). The first summand (the I-I-term) reads

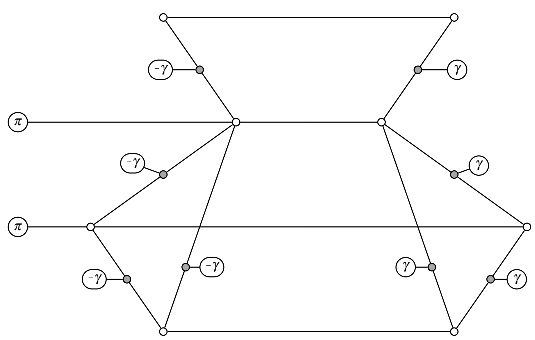

$$\overset{(f)}{=}$$

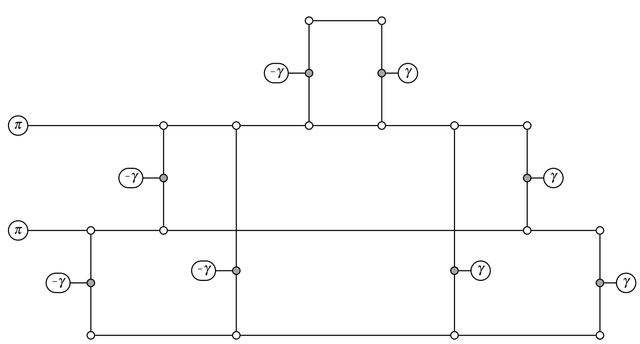

$$\overset{(8)}{=} \frac{1}{2^4}$$

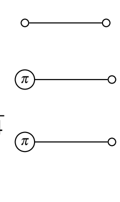

$$= \quad 0 \quad . \qquad (20)$$

The second summand (the I-X-term) reads

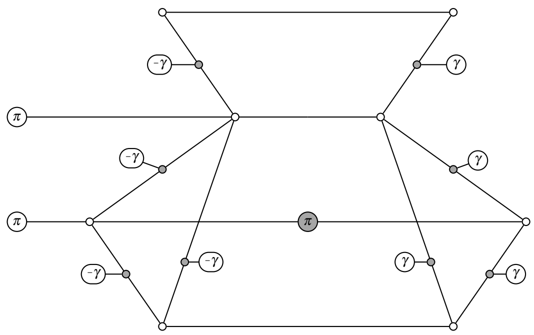

$\overset{(\pi)}{=}$

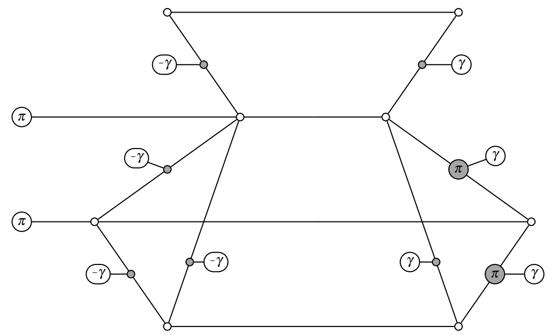

$\overset{(f)}{=}$

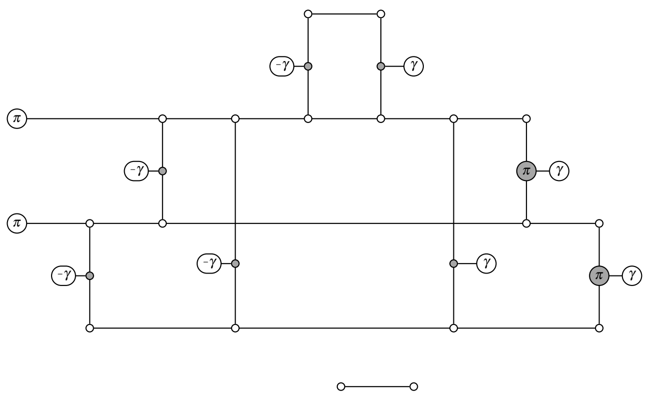

$\overset{(8)}{=} \dfrac{1}{2^2}$

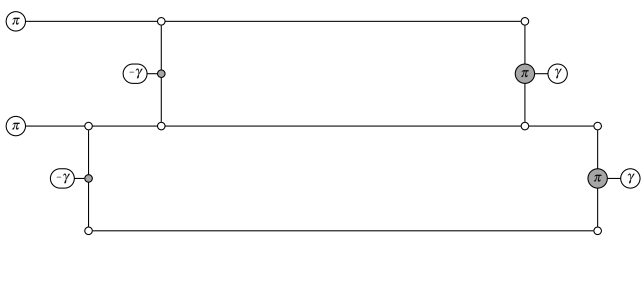

$= \dfrac{1}{2^2}$

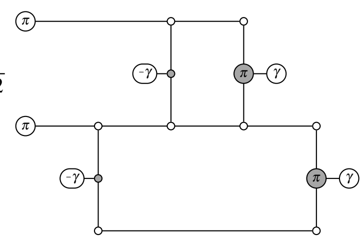

$\overset{(8)}{=} \dfrac{1}{2^3} \quad e^{2i\gamma}$

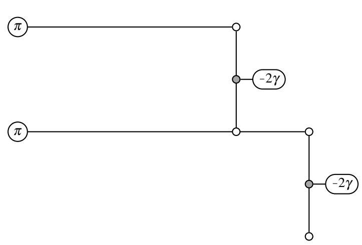

$\overset{(7)}{=} \frac{1}{2^4}$ 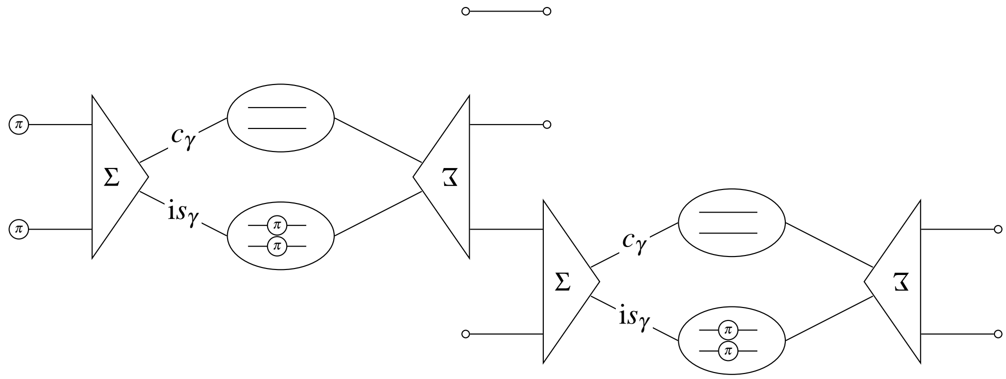

$\overset{(i)}{=} \frac{1}{2^4}$ 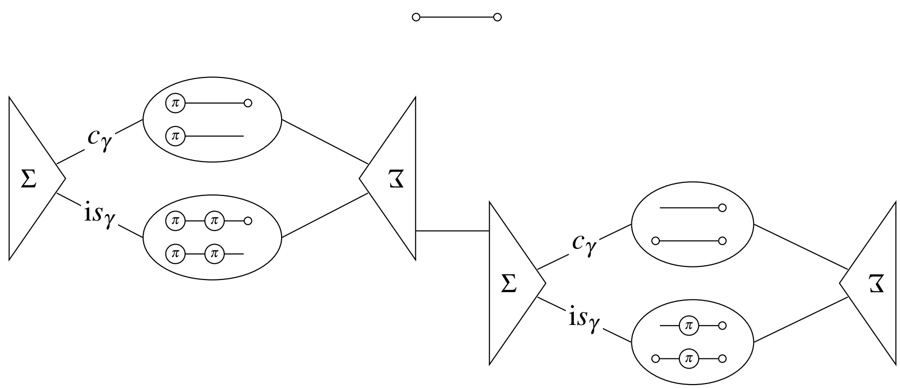

$\overset{(ii)}{=} \frac{1}{2^4} \quad \mathrm{i}s_\gamma c_\gamma$ 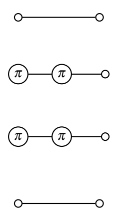 $= \quad \mathrm{i}s_\gamma c_\gamma$ (21)

.

The third summand (the *X*-*I*-term) reads

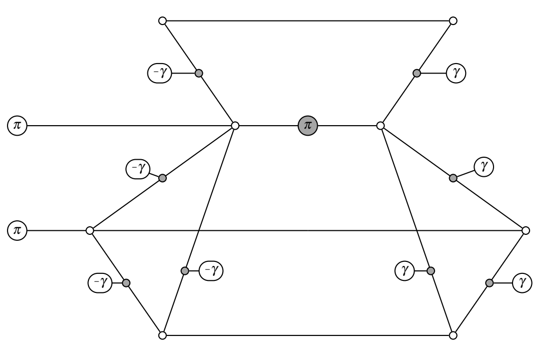 $\overset{(\pi)}{=}$ 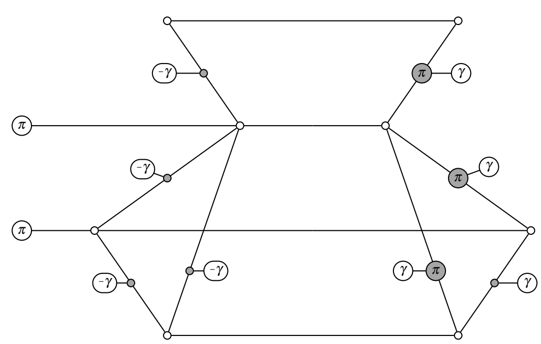

$\overset{(f)}{=}$

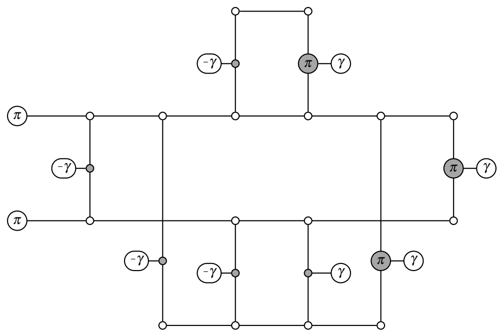

$\overset{(8)}{=} \frac{1}{2}$

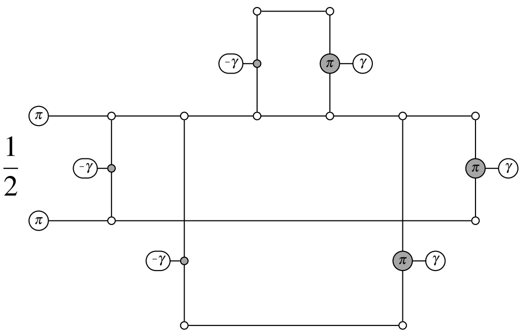

$= \frac{1}{2}$

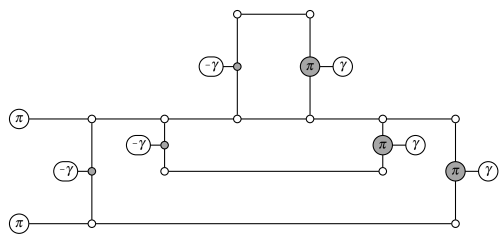

$\overset{(8)}{=} \frac{1}{\sqrt{2^5}} \; e^{3i\gamma}$

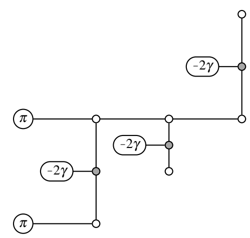

$\overset{(7)}{=} \frac{1}{2^4}$

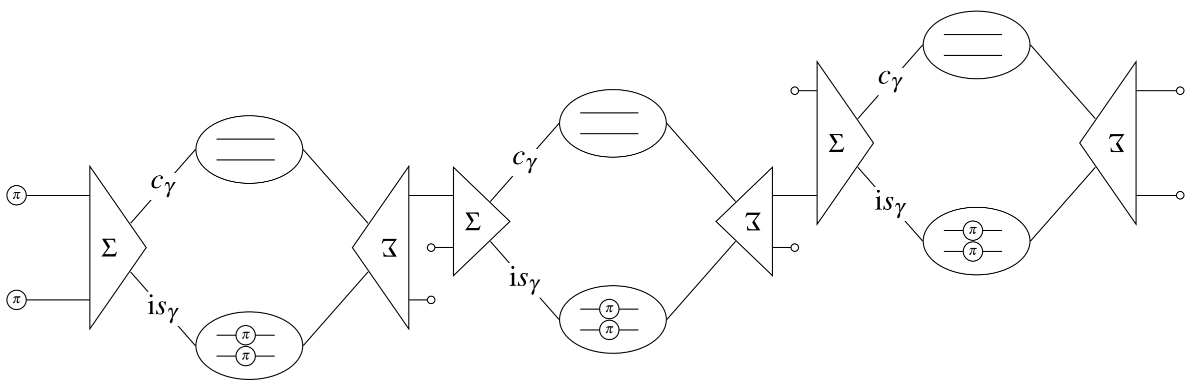

$\overset{(i)}{=} \frac{1}{2^4}$

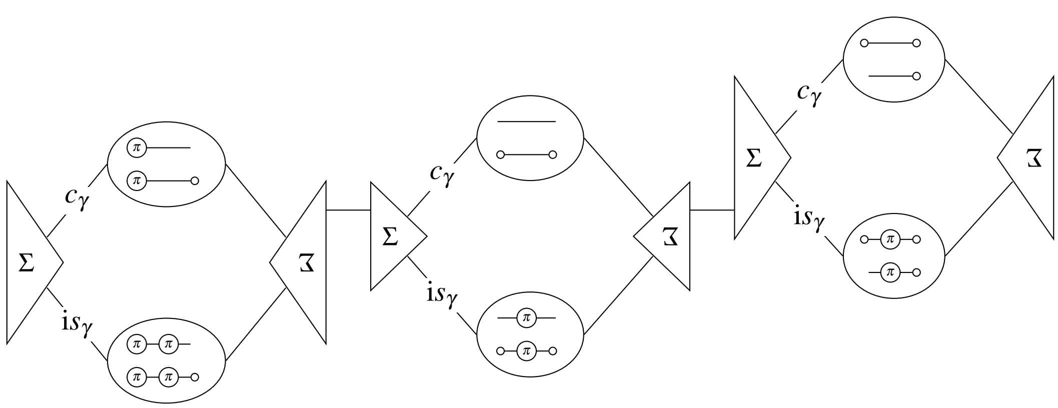

$$\overset{\text{(ii)}}{=} \frac{1}{2^4} \quad \mathrm{i} s_\gamma c_\gamma^2$$

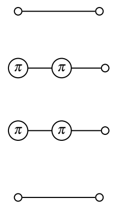

$$= \quad \mathrm{i} s_\gamma c_\gamma^2 \tag{22}$$

.

The fourth summand (the X-X-term) reads

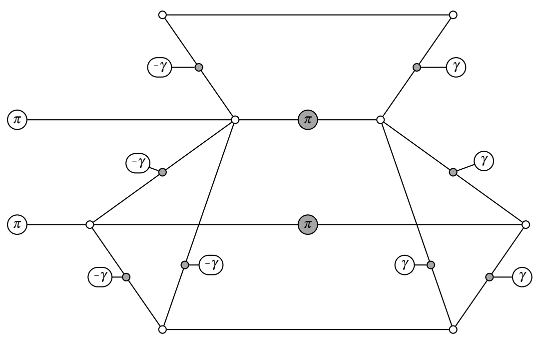

$$\overset{(\boldsymbol{\pi})}{=}$$

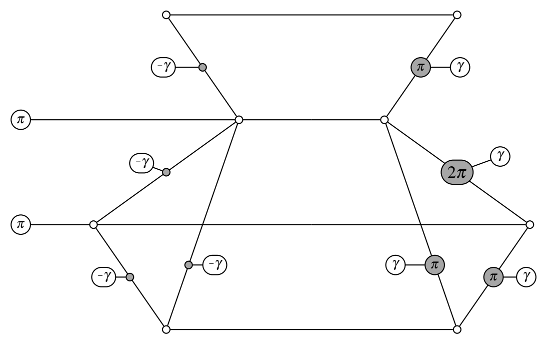

$$\overset{(\boldsymbol{f})}{=}$$

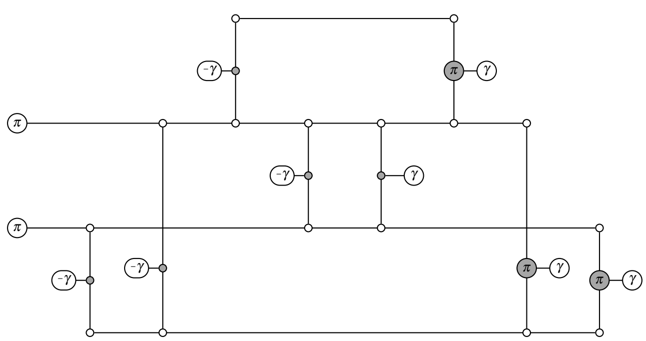

$$\overset{(8)}{=} \frac{1}{2}$$

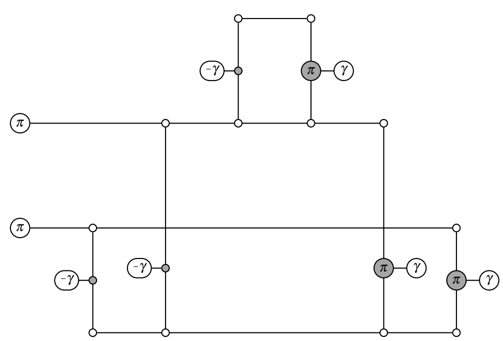

$$= \frac{1}{2}$$

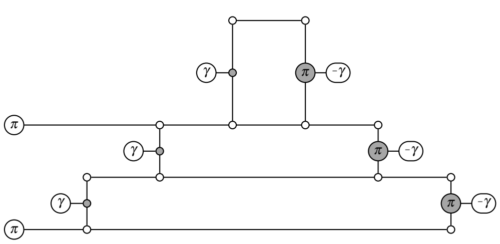

$$\overset{(8)}{=} \frac{1}{\sqrt{2^5}} \quad e^{3\mathrm{i}\gamma}$$

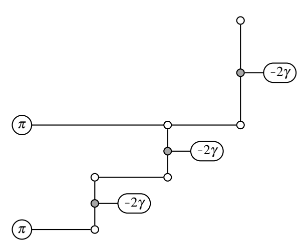

$\overset{(7)}{=} \frac{1}{2^4}$

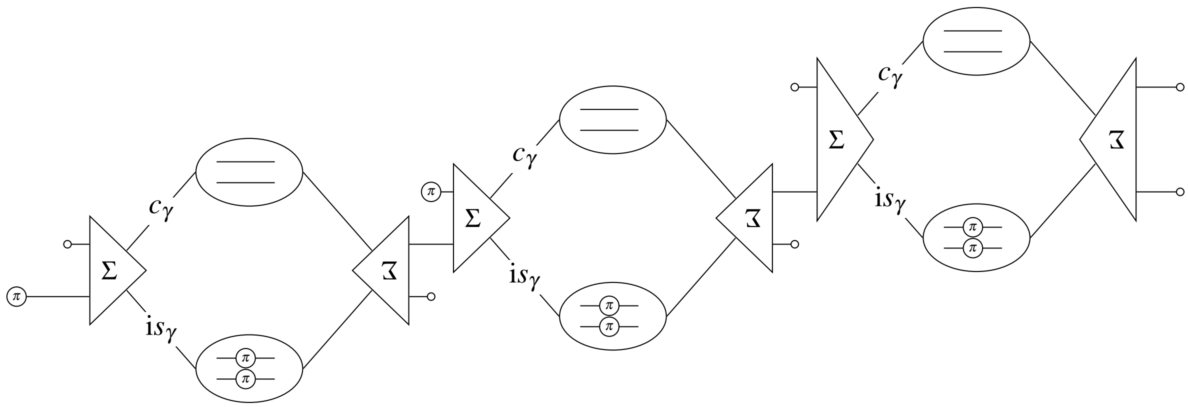

$\overset{(i)}{=} \frac{1}{2^4}$

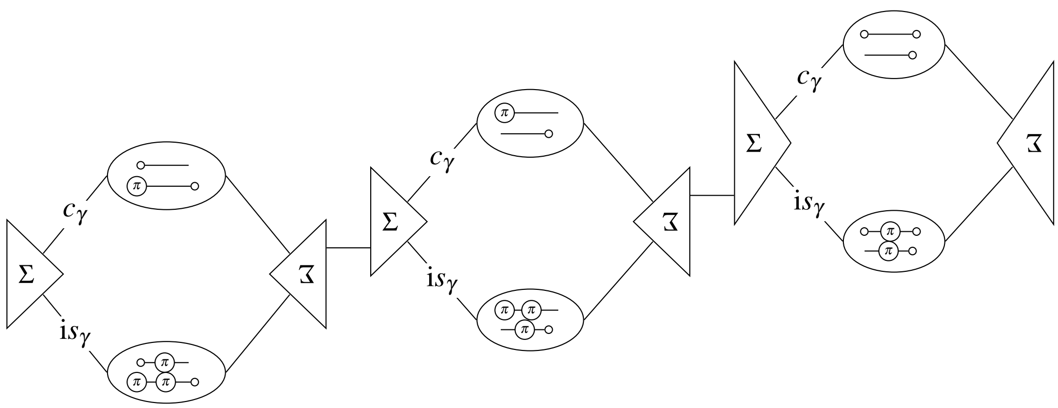

$\overset{(ii)}{=} \frac{1}{2^4} \quad (-s_\gamma^2 c_\gamma)$

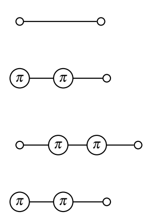

$= \quad -s_\gamma^2 c_\gamma \quad .$ (23)

D Proofs of useful ZX-diagram Identities

D.1 Phase-gadget identity

Proof of (8). First, we can us the spider fusion rule to write

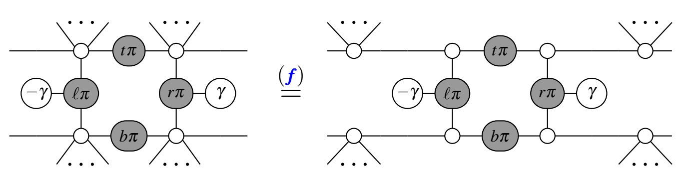

Then, we just consider the inner part

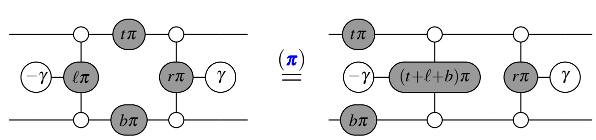

$\overset{(f)}{=}$ 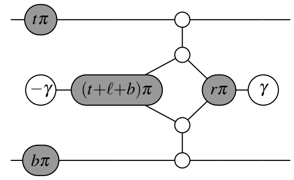

$=$ 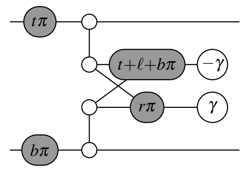

$\overset{(f)}{=}$ 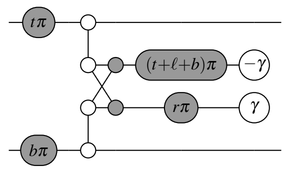

$\overset{(b)}{=} \frac{1}{\sqrt{2}}$ 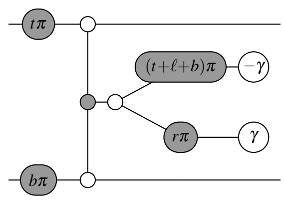

$\overset{(\pi)(f)}{=} \frac{1}{\sqrt{2}}$ 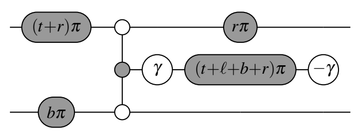 .

If $t+l+b+r$ even, we have

$\frac{1}{\sqrt{2}}$ 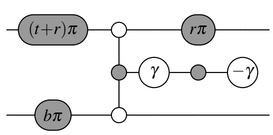 $\overset{(id),(f)}{=} \frac{1}{\sqrt{2}}$ 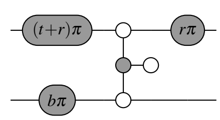

$\overset{(c)}{=} \frac{1}{2}$ 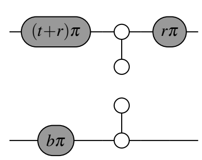

$\overset{(id),(f)}{=} \frac{1}{2}$ 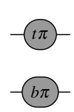 , else, if $t+l+b+r$ odd, we have

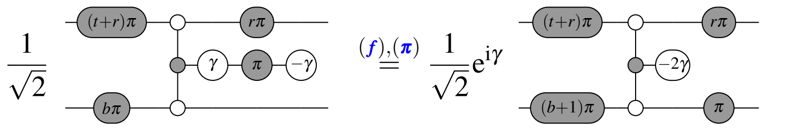

which proves (8). □

D.2 Hardware Efficient Ansatz

Proof of (17).

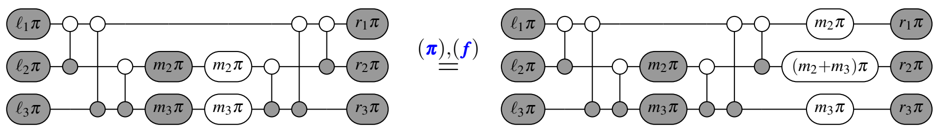

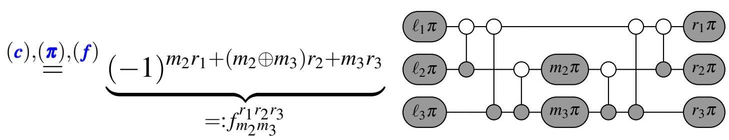

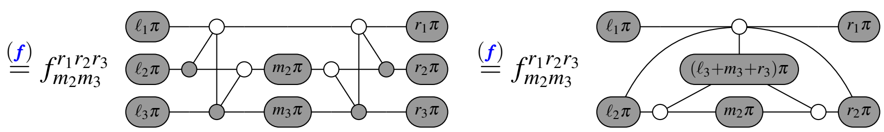

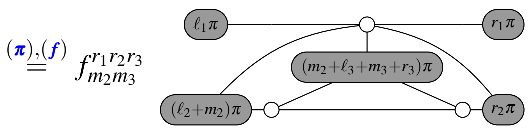

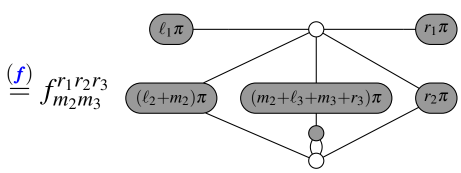

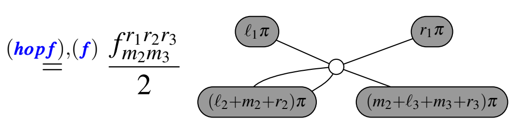

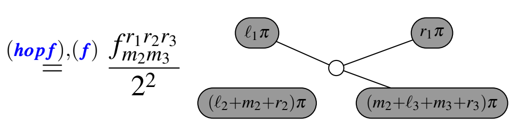

$$\overset{(c),(f)}{=} \frac{f^{r_1 r_2 r_3}_{m_2 m_3}}{2^3}$$

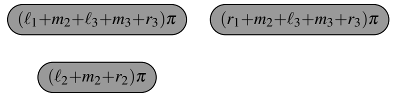

$\square$